PESQUISA VETERINÁRIA BRASILEIRA
Brazilian Journal of Veterinary Research
ISSN 0100-736X (Print)
ISSN 1678-5150 (Online)

Pesq. Vet. Bras. 41:e06894, 2021
DOI: 10.1590/1678-5150-PVB-6894

Topic of General Interest
Livestock Diseases

Shapes of pathology[1]

Raquel R. Rech[2]*, Paula R. Giaretta[3], Richard Ploeg[4], Erin E. Edwards[5], Corrie C. Brown[6] and Claudio S. L. Barros[7]

ABSTRACT.- Rech R.R., Giaretta P.R., Ploeg R., Edwards E.E., Brown C.C. & Barros C.S.L. 2021. **Shapes of pathology**. *Pesquisa Veterinária Brasileira 41:e06894, 2021*. Department of Veterinary Pathobiology, College of Veterinary Medicine & Biomedical Sciences, Texas A&M University, College Station, TX 77843-4467, USA. E-mail: rrech@cvm.tamu.edu

The shape is one of the key features of a lesion and a pathologist must be able to identify and interpret these forms in the context of any gross and microscopic changes. One of the principles of adult learning is to engage the learner with previously understood information. If, when presenting material that is new, a connection with something the student already has familiarity with, the learning process is accelerated. As the learners are already familiar with shapes they have encountered throughout their pre-pathology learning, these can be used to hasten the incorporation and understanding of lesions. This paper describes various shapes that are used in describing lesions in veterinary pathology.

INDEX TERMS: Pathology, veterinary pathology, shape analogies.

RESUMO.- [**As formas da patologia.**] A forma é uma das principais características de uma lesão. Um patologista deve ser capaz de identificar e interpretar essas formas no contexto de quaisquer alterações macroscópicas ou microscópicas. Um dos princípios da aprendizagem de adultos é envolver o aluno com informações previamente compreendidas. Se, ao apresentar um material novo, se estabelece uma conexão com algo que o aluno já conhece, o processo de aprendizagem torna-se mais rápido e eficiente. Como os alunos já estão familiarizados com as formas que encontraram ao longo de sua aprendizagem pré-patologia, elas podem ser usadas para acelerar a incorporação e a compreensão das lesões. Este artigo descreve várias formas que são usadas na descrição de lesões em patologia veterinária.

TERMOS DE INDEXAÇÃO: Patologia, patologia veterinária, analogia de formas.

INTRODUCTION

Shape describes the external form or contour of a material object or geometrical figure. Pathology is a unique medical specialty wherein, at baseline, education is imparted in both visual and experiential forms (Ahmed et al. 2019). Comparing lesions with common shapes or objects often makes the lesions easier to recognize and remember. The shapes inherent to a lesion often allow the pathologist to make interpretations as to its pathogenesis and hence facilitate the formulation of a morphologic or sometimes even an etiologic diagnosis. In this paper, we have compiled a list of shapes commonly coined as descriptors in veterinary pathology and we have attempted, where possible, to explain the pathogenesis that led to the formation of these shapes.

MACROSCOPIC FINDINGS

Integument and appendages

Paintbrush and strawberry footrot. The changes seen with cutaneous dermatophilosis, also known as "rain rot" or "rain scald" in cattle and "lumpy wool" in sheep, have been likened to paintbrushes (in Portuguese: *ponta de pincel*) and strawberry footrot in sheep. This translates literally into Portuguese as "pé podre em morango". Cutaneous dermatophilosis is seen worldwide in a wide range of

[1] Received on February 12, 2021.
Accepted for publication on May 5, 2021.
[2] Department of Veterinary Pathobiology, College of Veterinary Medicine & Biomedical Sciences, Texas A&M University, College Station, TX 77843-4467, USA. * Corresponding author: rrech@cvm.tamu.edu
[3] Escola de Veterinária, Universidade Federal de Minas Gerais (UFMG), Belo Horizonte, MG 31270-901, Brazil.
[4] Faculty of Veterinary and Agricultural Science, University of Melbourne, 250 Princes Highway, Werribee, Vic 3030, Australia.
[5] Texas A&M Veterinary Medical Diagnostic Laboratory, College Station, TX 77843-4471, USA.
[6] The University of Georgia, College of Veterinary Medicine, Department of Pathology, 501 D.W. Brooks Drive Athens, Georgia 30602, USA.
[7] Faculdade de Medicina Veterinária e Zootecnia, Universidade Federal de Mato Grosso do Sul (UFMS), Av. Senador Filinto Müller 2443, Campo Grande, MS 79074-460, Brazil.

domestic and wild animal species (Mauldin & Peters-Kennedy 2016). It is prevalent in humid, tropical and subtropical areas (Mauldin & Peters-Kennedy 2016). The disease is caused by *Dermatophilus congolensis*, an aerobic and facultatively anaerobic gram-positive bacterium which produces zoospores (Zaria & Amin 2004). Climatic conditions (high humidity and rainfall) play an important role in bacterial activation (Zaria & Amin 2004). Predisposing factors to infection include skin damaged either by trauma (prickly vegetation) or ectoparasites, particularly ticks or insect bites (Mauldin & Peters-Kennedy 2016). Transmission occurs by direct or indirect contact (Mauldin & Peters-Kennedy 2016). Grossly, the lesions consist of papular to exudative crusting dermatitis, especially along the dorsum (Mauldin & Peters-Kennedy 2016). In calves, the lesions often occur on the muzzle, neck and head (Mauldin & Peters-Kennedy 2016). The formation of scabs and moist exudate lead the hair or fleece to clump and glue together forming firm to hard spikes called paintbrushes (Zaria & Amin 2004, Mauldin & Peters-Kennedy 2016). They can easily break off and resemble the bristles of an artist's brush (Fig.1). *Dermatophilus congolensis* infection in combination with contagious viral pustular dermatitis (orf) has been implicated in strawberry footrot in sheep. These lesions are exuberant, proliferative, red masses on the distal limbs resembling mashed strawberries (Scott 2018).

Tree bark. Photosensitization dermatitis occurs in animals when photodynamic pigments deposited in the skin are exposed to sunlight (Cullen & Stalker 2016). These pigments absorb ultraviolet light and convert it to longer wavelength light, usually beyond the ultraviolet B range (Mauldin & Peters-Kennedy 2016). The energy of the absorbed light causes necrosis of tissues exposed to sunlight (Mauldin & Peters-Kennedy 2016). Initially this manifests as erythema but soon progresses to edema and extensive necrosis, distributed especially in areas that lack pigmentation or hair (Mauldin & Peters-Kennedy 2016). The surface of the necrotic skin becomes dry and peels off (Giaretta et al. 2014) as desiccated plates that resemble the bark of a tree (in Portuguese: *casca de árvore*) (Fig.2).

There are three types of photosensitization based on the source of the photodynamic pigments (Mauldin & Peters-Kennedy 2016). In primary photosensitization (type I), the source of photodynamic pigment is plants or drugs (Mauldin & Peters-Kennedy 2016). As a result, herbivores are the most frequently affected species (Chen et al. 2019). After absorption from the gastrointestinal tract, these agents travel via the portal circulation, are incompletely removed by the liver, and hematogenously spread to skin capillaries. In Brazil, the main plants causing primary photosensitization include *Ammi majus*, *Froehlichia humboldtiana* (Tokarnia et al. 2012b) and *Malachra fasciata* (Araújo et al 2017). In the United States, outbreaks of primary photosensitization have been associated with consumption of *Ammi majus* and alfafa hay (*Medicago sativa*) (Chen et al. 2019). In Australia various species of *Hypericum* (St John's wort) are also implicated (Seawright 1982).

Type II photosensitization is associated with genetic disorders that compromise the metabolism of the heme pigment (Mauldin & Peters-Kennedy 2016, Varaschin et al. 1998). This disorder results in the accumulation of hematoporphyrins in tissues (Mauldin & Peters-Kennedy 2016). The main diseases are bovine erythropoietic protoporphyria reported in Limousin and Holstein-Friesian cattle and bovine hematopoietic porphyria reported in Shorthorn, Holstein-Friesian, and Hereford cattle (Mauldin & Peters-Kennedy 2016).

Phytoporphyrin (formerly phylloerythrin) is the photodynamic pigment involved in hepatogenous (type III) photosensitization (Cullen & Stalker 2016). With disorders of liver function the compromise in the clearance of phytoporphyrin, the degradation product of chlorophyll, and its resultant accumulation in the tissues, produces this syndrome (Cullen & Stalker 2016). In Brazil, several plants are associated with hepatogenous photosensitization including *Brachiaria* spp., *Lantana* spp., *Panicum dichotomiflorum*, *Myoporum laetum*, *Enterolobium gummiferum, Enterolobium contortisiliquum* and *Senecio* spp. (Tokarnia et al. 2012a, Leal et al. 2017, Panziera et al. 2017). The mycotoxin sporidesmin, produced by the fungus *Pithomyces chartarum*, and toxic plants including *Lantana camara* (Morton 1994), *Panicum coloratum* (kleingrass), among other *Panicum* species are reported as causes for hepatogenous photosensitization in the United States (Chen et al. 2019). In Australia, secondary photosensitization is often associated with hepatic damage caused by *Panicum effusum*, *Panicum laevifolium*, *Tribulus terrestris*, *Heliotropium europaeum*, *Echium plantagineum* and *Lantana camara* as well as the mycotoxins from *Pithomyces chartarum* and *Phomopsis leptostromiformis* (Chen et al. 2019). The blue-green algae, *Anacystis cyanea*, is also occasionally implicated (Beasley et al. 1989).

Diamond skin disease. Slightly raised, red, rhomboid or diamond-shaped areas on the haired skin predominantly around the abdomen and thighs are classic lesions of the septicemic form of swine erysipelas (in Portuguese: *pele em diamante*) (Mauldin & Peters-Kennedy 2016) (Fig.3). The causative agent is *Erysipelothrix rhusiopathiae*, a facultative intracellular gram-positive rod (Mauldin & Peters-Kennedy 2016). Piglets less than three months of age and pigs older than three years of age are least predisposed to erysipelas (Mauldin & Peters-Kennedy 2016). In the early septicemia, the bacteria lodges in vessels, leading to vasculitis, thrombosis and acute infarcts (Opriessnig & Coutinho 2019). The rhomboid nature of the skin lesion may be related to the area of skin served by a particular vessel in swine (Zhang et al. 2000), as other septicemic conditions may cause similar, but less pronounced rhomboid skin lesions. As the disease progresses, the skin becomes dark, dry and partially detaches from the underlying dermis (Opriessnig & Coutinho 2019). If the pig survives, the lesions disappear in four to seven days (Opriessnig & Coutinho 2019). The main differential diagnosis for multifocal, well-circumscribed, slightly raised, dark red areas mainly in the ventrum, groin and thighs is porcine dermatitis nephropathy syndrome (PDNS), which is strongly associated with porcine circovirus-2 (PCV-2) (Segales 2012) or PCV-3 infection (Jiang et al. 2019). In PDNS, the lesions are irregular to circular and do not appear rhomboid as in swine erysipelas (Segales 2012). *Actinobacillus suis* infection also rarely causes rhomboid lesions in the skin (Opriessnig & Coutinho 2019).

Lechiguana. Lechiguana is a colloquial name of a disease in cattle in Southern Brazil characterized as a proliferative fibrogranulomatous panniculitis caused by infection with *Mannheimia granulomatis* (Riet-Correa et al. 1992, Ladeira 2007). The panniculitis evolves as a dense, hard, rapidly growing mass associated with lymphadenopathy (Riet-Correa et al. 1992). Affected cattle become emaciated and, if left untreated, die

Fig.1-6. (**1**) Multifocal to coalescing, subacute exudative and hyperkeratotic dermatitis; haired skin; bovine. Disease: dermatophilosis. Shape analogy: Paintbrush. Multifocal to coalescing, firm, 0.2-2.5cm thick, brown to gray crusts with entrapped hair. Inset: when the firm to hard spikes are pulled off, they resemble the bristles of an artist's brush. (**2**) Locally extensive, subacute, necrotizing and serocellular dermatitis; muzzle; bovine. Etiology: hepatogenous (type III) photosensitization due to *Senecio* sp. Shape analogy: Tree bark. Necrosis of the skin of the muzzle sloughs off as the dried barks of a tree. (**3**) Multifocal to coalescing, acute vasculitis with rhomboid infarcts; haired skin; swine. Shape analogy and name of the disease: Diamond skin disease. The red square areas resemble diamonds and are highly suggestive of acute infection of *Erysipelothrix rhusiopathiae*. Photo courtesy: Dr. Joaquim Segales, Universitat Autonoma de Barcelona. (**4**) Locally extensive, chronic, proliferative, fibrogranulomatous panniculitis; prescapular region; bovine. Etiology: *Mannheimia granulomatis.* Shape analogy and name of the condition: Lechiguana. Inset: wasp nest mimicking the shape of the subcutaneous lesion of lechiguana. Photo courtesy: Dr. Franklin Riet-Correa, Universidade Federal da Bahia. (**5**) Alopecia; tip of the tail; bovine. Etiology: ingestion of the mushroom *Ramaria flavo-brunnescens*. Shape analogy: Rat tail. (**6**) Locally extensive subcutaneous edema; submandibular region; bovine. Etiology: hypoproteinemia due to endoparasitism. Shape analogy: Bottle jaw.

within 3-11 months. In two months, the fibrogranulomatous mass may reach 55x40x10cm (Riet-Correa et al. 1992) (Fig.4).

Lechiguana is a colloquial name given to honey-producing spider wasps (tribe Persini) or the nests built by those wasps (inset Fig.4). The striking similarities between the shape of the wasps' nest and the large pyogranulomatous inflammatory mass induced by *M. granulomatis* gave origin to the popular name of lechiguana to the lesion and disease.

Rat tail. Hair loss of the entire length or the tip of the tail of animals is commonly called rat tail (in Portuguese: *cauda de rato*) (Mauldin & Peters-Kennedy 2016). In dogs, hypothyroidism is a classic endocrine disease where decreased levels of thyroid hormones do not stimulate the anagen stage of the hair cycle, and therefore, there is an increased relative proportion of telogen follicles with hair loss leading to alopecia (Gross et al. 2005a). In cattle, alopecia of the tail has been described in alkali disease (O'Toole & Raisbeck 1995), in a congenital and inherited disorder of hypotrichosis called "rat-tail" syndrome (RTS) (Knaust et al. 2016), and *Ramaria flavo-brunnescens* toxicosis (Fig.5) (Barros et al. 2006). In alkali disease, caused by prolonged oral exposure of cattle to elevated dietary selenium, a defective keratinization results via low amounts of sulphur containing amino acids (cystine) in hard keratin structures leading to dyskeratosis of the hair shafts and dystrophic hooves (O'Toole & Raisbec 1995). Similarly, in *Ramaria flavo-brunnescens* poisoning, defective keratinization has been shown in the keratinized structures, mostly in the hard keratin (Trost et al. 2009). In RTS, the defect in hair conformation is restricted to the pigmented areas of hair coat and occurs in crosses between black cattle breeds (e.g., Angus and Holstein) and some European breeds that are characterized by color dilution of the coat (e.g., Simmental, Charolais and Hereford) (Knaust et al. 2016).

Bottle jaw. In ruminants, hypoproteinemia can manifest as subcutaneous edema of the submandibular and cervical area, producing a swollen, bottle-shaped aspect (Fig.6) and hence the name "bottle jaw" (Bowman 2014). This translates literally into Portuguese as "queixada de garrafa". However, the condition bottle jaw is colloquially known in Brazil as "papeira".

Hypoproteinemia can result from decreased protein intake, malabsorption and/or gastrointestinal loss (Uzal et al. 2016). Marked hypoalbuminemia leads to decreased osmotic pressure and development of edema in the subcutaneous tissue, mesentery, gastric mucosa and within the body cavities (Uzal et al. 2016). The "bottle jaw" aspect is commonly observed in ruminants with severe gastrointestinal parasitism such as ostertagiasis, haemonchosis and fascioliasis (Myers & Taylor 1989, Bowman 2014).

Kunkers and leeches. Kunkers (the same denomination is used in Portuguese) are structures typically associated with *Pythium insidiosum* infection in horses. They are rigid, tubular, 2-10 millimeters in diameter gray-white to a pale yellow detachable, firm to friable coral-like structures with irregular surfaces (Fig.7). In horses, the coral-like structures of pythiosis are distinctively larger than those seen amidst the lesions caused by *Basidiobolus* spp. and *Conidiobolus* spp. (Miller & Campbell 1984).

The well-developed lesions of equine pythiosis consist of masses of granulation tissue crisscrossed by fistulous sinus tracts containing the kunkers (Martins et al. 2012). Histologically, the kunkers are composed of coagulative necrosis, necrotic eosinophils and *Pythium* hyphae. A thick viscous exudate oozes from the fistulous tracts (Mauldin & Peters-Kennedy 2016). These masses were called kunkers originally in India (Datta 1933). These structures were likened to a type of limestone formation seen in southern India and known by the Sanskrit word, kunker (Newbold 1846). As such, the concretions were referred to as 'kunkur stones' (Smith 1879).

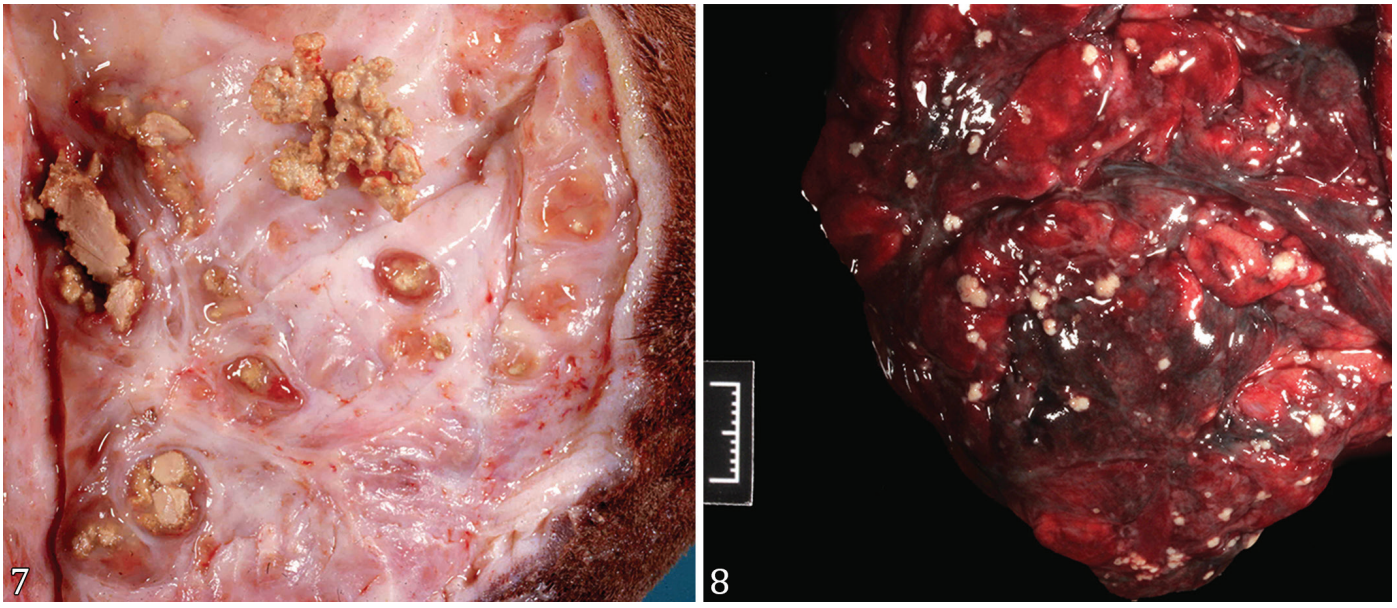

Fig.7-8. (**7**) Multifocal to coalescing, chronic, granulomatous and eosinophilic cellulitis; equine. Etiology: *Pythium insidiosum*. Shape analogy: Kunkers. Photo courtesy: Dr. Roger Kelly, University of Queensland, Australia. (**8**) Multifocal to coalescing, chronic, pyogranulomatous omentitis; omentum; canine. Etiology: *Nocardia* sp. Shape analogy: Sulfur granules. Histologically, the pale tan to yellow, granules seen on the surface of the red and thick omentum contain colonies of branching filamentous bacteria surrounded by Splendore-Hoeppli deposits and inflammatory cells.

The same condition (under the name of "horse-leech") was described in Florida (USA), where the structures - elsewhere known as kunkers - were named leeches (in Portuguese: *sanguessuga*). The reason for this was probably the elongate masses oozing viscous exudate resembled aquatic leeches (Thompson & Young 1896, Bridges & Emmons 1961). It makes sense since frequently affected areas of the equine body affected by cutaneous pythiosis most likely to be in prolonged contact with water in lakes, ponds, swamps, or flooded areas are the ventral thorax, abdomen and limbs. (Mauldin & Peters-Kennedy 2016).

Sulfur granules. Grossly, the incorporation of colonies of organisms amidst Splendore-Hoeppli deposits can contribute to the formation of yellowish grains or granules (Fig.8) visible within exudates leeching from draining fistulous tracts or body cavity fluids. These are referred to as sulfur granules (in Portuguese: *grãos de enxofre*) in association with *Actinomyces* spp. infections and similar granules can be seen less often with *Nocardia* spp. (Gross et al. 2005b). Granules can on occasion be seen within the exudates of bacterial pseudomycetoma/botryomycosis (Gross et al. 2005b). Tissue grains are also evident within exudates from fungal infections such as dermatophytic pseudomycetoma and eumycotic mycetoma (pigmented and non-pigmented) (Gross et al. 2005b). Dependent upon the inciting organism, it and its associated Splendore-Hoeppli deposits are accompanied by an inflammatory reaction varying in composition and intensity incorporating neutrophils, eosinophils, epithelioid macrophages and giant cells. Occasionally, this reaction is seen in the midst of wide areas of degeneration and necrosis.

Digestive system

Wave mouth. Wave mouth (in Portuguese: *oclusão em onda*) is seen commonly in aged horses and is characterized by an undulating, wave-like contour of the occlusive surfaces of the cheek teeth (Fig.9) (Anthony et al. 2010). Affected teeth have drastic differences in height, and the upper and lower arcades have inverse wave patterns. In most cases, there is severe attrition of some teeth. Wave mouth is a chronic condition caused by uneven growth and uneven wear of the molar and premolar cheek teeth (Uzal et al. 2016). It can usually be prevented with regular dental care and floating. Wave mouth severely restricts movement of the teeth, impeding mastication and leading to weight loss, malnutrition, and poor body condition. This condition is also a risk factor for colonic impaction in horses.

Serpiginous tracks. Serpiginous, zig-zag or ribbon-candy tracks (in Portuguese: *trajeto serpiginoso* or *em zigue-zague*) is a typical incidental finding on the esophageal mucosa due to migration of *Gongylonema* sp. (Fig.10), mostly in ruminants and swine (Uzal et al. 2016), and less commonly in donkeys, primates, humans (Libertin et al. 2017) as well as other captive exotic species (Craig et al. 1998). The definitive host acquires the infective larvae by accidental ingestion of cockroaches or dung beetles (intermediate hosts). The female nematodes are thin, approximately 25-30mm long, with a diameter of 0.25-0.5mm. The anterior end of the worm is notable for a short esophagus and characteristic longitudinal rows of cuticular bosses or scutes. Their migration through the esophageal mucosa incites little inflammation and it is mostly harmless for the definitive host. Histologically, *Gongylonema* sp. are characterized by polymyarian-coelomyarian musculature, large cervical alae with cuticular bosses on the anterior end, asymmetrical lateral cords, and small, thick-shelled, embryonated eggs (Eberhard 2014).

In sheep, migrating larvae of *Cysticercus tenuicollis* (Corda et al. 2020) and immature flukes of *Fasciola hepatica* (Cullen & Stalker 2016) cause serpiginous tracks in the liver parenchyma. The serpiginous tracks represent acute traumatic lesions caused by the wandering of immature helminths. The streaks or foci are either dark red or light yellow, varying from alternating areas of hemorrhage and necrosis or infiltrated by inflammatory cells (Cullen & Stalker 2016).

Barber's pole. Whilst not representing a pathologic lesion, we felt it important to include *Haemonchus* spp. (*H. contortus*, *H. placei* and *H. similis*) in this discussion due to the usefulness of this analogy during ruminant necropsy. *H. contortus* lives in the abomasum of cattle and small ruminants or analogous 3rd gastric compartment of camelids. It is less frequently seen in deer and exotic ruminants (Edwards et al. 2016). The common name of this parasite is barber's pole worm (in Portuguese: *poste de barbeiro*), a nickname that helps differentiate it from other gastric parasites.

The origin of the term barber's pole is said to derive from the Middle Ages when barbers performed more than just haircuts. In those times, barbers used their blades to perform other minor surgical procedures including blood-letting. It is said that the red stripe on the barber's pole represents blood and the white stripe represents linen bandage material. During this procedure, patients were given a staff to grip so that their veins would be more prominent and accessible. Some barbers would wrap blood-stained linens around this staff and place it outside of their establishment as a symbol of their services (Whitaker et al. 2004). Barber's pole in Europe have a red and white spiral twist, whereas in North America, barber poles also have an added blue stripe. Multiple theories exist for the later addition of the blue stripe. Some suggest it represents a vein, while others believe it to be a symbol of patriotism.

Ironically, the red twisted stripe seen in *H. contortus* parasites also represents blood. These parasites feed on whole blood from the host, and the parasites' blood-filled intestinal tract can be seen with the naked eye. The white stripe is only seen in female *H. contortus* specimens and corresponds to the egg-filled uterus that is wrapped around the intestine. Males appear as solid red or tan nematodes, depending on how much blood is in their intestine, and females exemplify the classic barber pole shape (Fig.11).

Accordion-folded intestine. Gastrointestinal foreign bodies are common findings during the necropsy of cats and dogs. Non-linear foreign bodies usually lodge in the lumen and cause obstruction of the gastrointestinal tract. Linear foreign bodies, mainly string, often are tethered proximally around the base of the tongue or in the pylorus (Hobday et al. 2014). If a length of these extend into the intestine, the normal peristaltic movements will result in plication of this segment of bowel around the immovable intraluminal foreign body (Fig.12). From the serosal surface, the pleating of the intestine gives the characteristic appearance of folded bellows of the accordion (in Portuguese: *fole de acordeão, gaita ou sanfona*). On the mucosa of the affected small intestine, linear erosions to transmural ulcerations are common along the

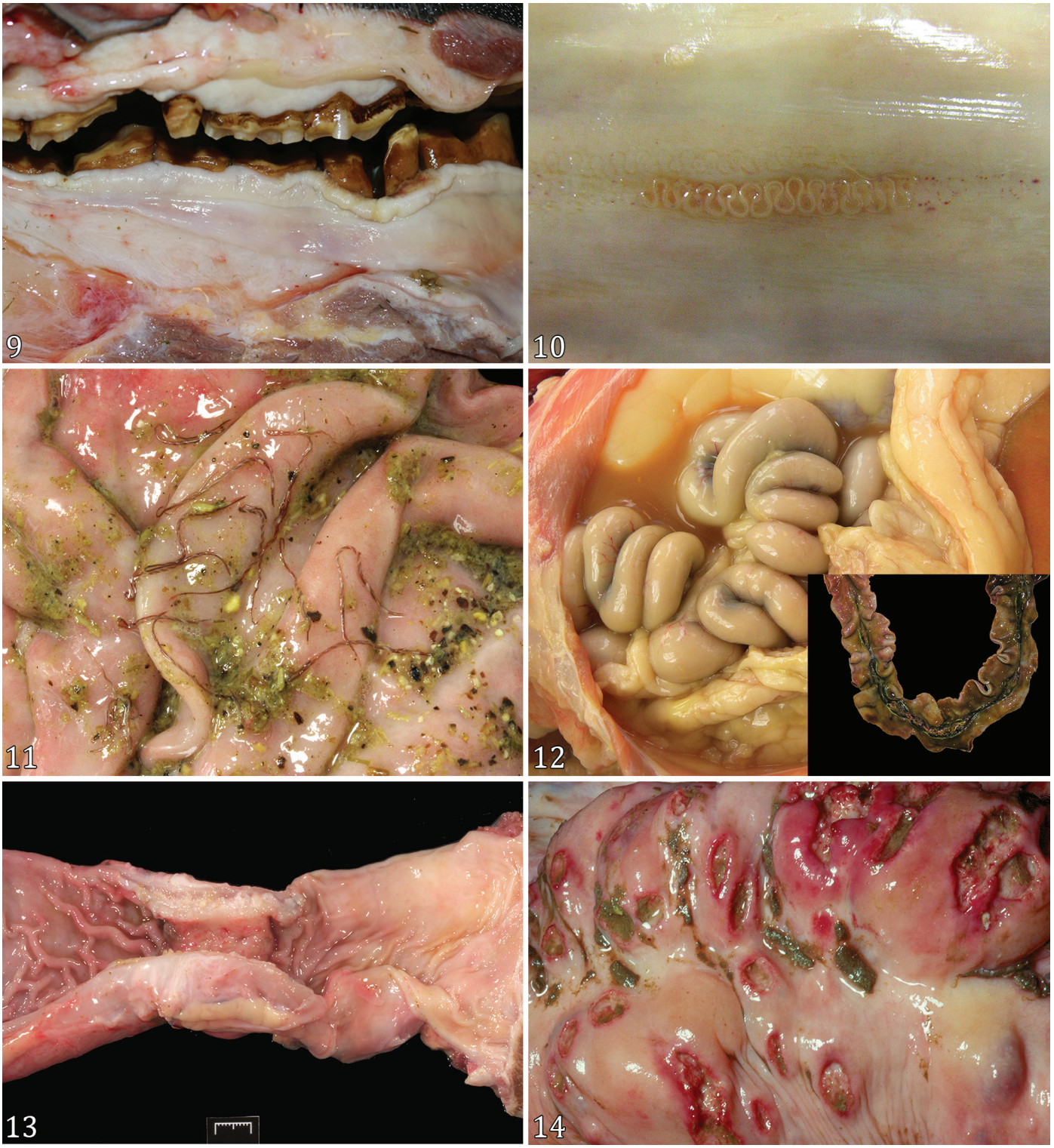

Fig.9-14. (**9**) Uneven growth and wear; molar and premolar teeth; equine. Shape analogy: Wave mouth. The undulating appearance of the occlusive surfaces of the cheek teeth leads to poor mastication and impaction of the large colon. (**10**) Esophageal gongylonemiasis; bovine. Etiology: *Gongylonema pulchrum*. Shape analogy: Serpiginous tracks. (**11**) Abomasal haemonchosis; caprine. Etiology: *Haemonchus contortus*. Shape analogy: Barber's pole. The red and white stripe corresponds to the egg-filled uterus that is wrapped around the intestine containing blood. (**12**) Plicated small intestine; feline. Shape analogy: Accordion-folded intestine. The plicated intestine indicates an intraluminal linear foreign body. Inset: linear mucosal ulceration along the mesenteric border due to linear foreign body in a dog. (**13**) Colonic adenocarcinoma; canine. Shape analogy: Napkin-ring stricture has resulted in partial obstruction of the intestinal lumen. (**14**) Pyogranulomatous colitis; large colon; equine. Etiology: *Rhodococcus equi*. Shape analogy: Crateriform. The mucosa is randomly elevated by contains semi-confluent nodules with a craterous ulcerated center. Photo courtesy: Dr. Roger Kelly, University of Queensland, Australia.

mesenteric border (inset Fig.12), which may lead to intestinal perforation and peritonitis.

Napkin-ring stricture. The scirrhous response (fibrosis) associated with choke, esophageal squamous cell carcinomas or intestinal adenocarcinomas often leads to annular thickening and stricture of the intestinal wall with associated luminal stenosis. Orad to this narrowing, the digestive tube expands above to its normal diameter. As such, this affected length of intestine resembles a serviette positioned in a napkin ring (in Portuguese: *anel de guardanapo*) (Fig.13).

In horses, the circumferential mucosal damage secondary to choke contributes to the esophageal stricture. Cattle feeding for years on pastures with high levels of contamination with bracken fern (*Pteridium arachnoideum*) may develop squamous cell carcinoma of the upper digestive tract, including an annular stenotic thickening of the esophageal wall (Faccin et al. 2017). Adenocarcinomas are the second most common intestinal neoplasm of cats and the most common intestinal neoplasm of the other domestic species. German shepherds, collies, Siamese cats and Arabian horses are overrepresented (Munday et al. 2017). Intestinal adenocarcinomas are present in 7% of old, unthrifty sheep in New Zealand (Munday et al. 2006).

Crateriform. In human pathology, crateriform or craterous (in Portuguese: *crateriforme*) is often used to describe dome-shaped cutaneous epithelial neoplasms which incorporate a central crater. They are typically an exo-endophytic, cup-shaped lesion with central accumulations of keratin. Examples of such lesions include the keratoacanthoma, variants of squamous cell carcinoma and even forms of Bowenoid *in situ* carcinoma (Misago et al. 2013).

In veterinary pathology, crateriform is used for lesions of elevated margins with a central necrosis or ulceration. Ulcerated keratoacanthomas in broiler chickens have a crater-like appearance. They are spontaneously regressing neoplasms adjacent to the feather follicles, most commonly observed at processing after feathers have been removed (Abdul-Aziz & Barnes 2018a). The pyogranulomatous enterotyphlocolitis of *Rhodococcus equi* in foals is characterized by multifocal, 1-2cm in diameter, elevated, crateriform mucosal and submucosal nodules (Fig.14). The enteric lesions in foals with pneumonia is thought to be a consequence of swallowing of respiratory exudate containing *R. equi* (Uzal & Diab 2015).

Button ulcers. The chronic forms of classical swine fever (CSF) and salmonellosis in pigs and less frequently chronic salmonellosis in cattle (Njaa et al. 2012) and horses can manifest as round ulcers with raised edges rimmed by fibrosis in the mucosa of the ileocecal valve and colon. These are called button ulcers (in Portuguese: *úlceras botonosas*) (Fig.15) (Uzal et al. 2016, Valli et al. 2016).

Classical swine fever is a transboundary animal disease of domestic pigs and notifiable to the OIE World Organization for Animal Health. The main hosts for classical swine fever virus (CSFV) are domestic pigs (*Sus scrofa domesticus*) and European wild boars (*Sus scrofa scrofa*). Pestiviruses, such as CSFV, may act as a Trojan horse when sows are infected between days 50 and 70 of pregnancy, with persistently infected offspring. These piglets seem to be healthy, but die due to chronic forms. The lesions of the chronic form consist of atrophy of the thymus, lymphoid depletion and necrosis of the gut-associated lymphoid tissue, leading to the formation of button ulcers (Blome et al. 2017).

Infection by *Salmonella* Cholerasuis in pigs leads to septicemia and later to button ulcers in the colonic mucosa due to preferential localization of the bacterium in M cells of Peyer's patches (Uzal et al. 2016), again a lymphoid predilection.

Pearls. Dissemination of bovine tuberculosis to the pleura, peritoneum or pericardium produces multiple tubercles with 0.5-1 cm in diameter that grossly resemble pearls (Fig.16). This is referred to as "pearly disease" (Atkinson et al. 1909) or "tuberculous pearls" (in Portuguese: *tuberculose perlada*). Bovine tuberculosis is a chronic and zoonotic disease caused by *Mycobacterium bovis* in most of the cases (Domingo et al. 2014). Recognition of characteristic gross lesions during meat inspection is crucial for surveillance and control of bovine tuberculosis in herds (Domingo et al. 2014). Lesions may be localized, affecting primarily the lungs and draining lymph nodes, or can be generalized (Domingo et al. 2014). The generalized form of tuberculosis can result from deficient immune response, disease progression

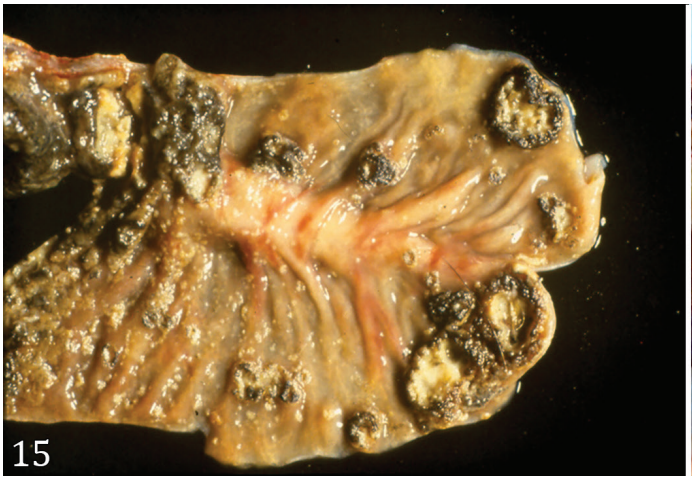

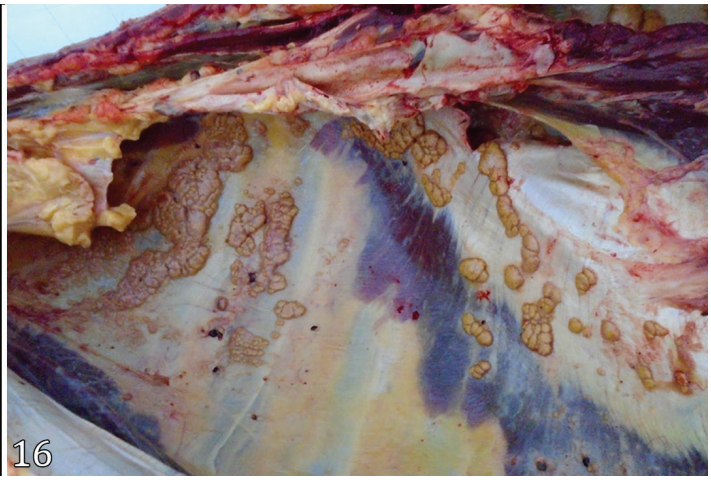

Fig.15-16. (**15**) Multifocal, ulcerative typhlitis; cecum; swine. Disease: classical swine fever. Shape analogy: Button ulcers are a characteristic macroscopic finding for chronic classical swine fever and enteric salmonellosis. Photo courtesy: Dr. Murilo Nogueira dos Santos. (**16**) Multifocal to coalescing, chronic, granulomatous pleuritis; pleura; bovine. Disease: tuberculosis. Shape analogy: Tuberculous pearls. Serosal generalization of tuberculous granulomas may resemble pearls. Photo courtesy: Dr. Ingrid Saccol Wiethan.

or reinfection, via hematogenous or lymphatic dissemination (Domingo et al. 2014). Miliary tuberculosis is the most common manifestation of generalized infection and consists of countless, gray to white-yellow, poorly demarcated foci of caseous necrosis in the lungs and other organs (Domingo et al. 2014). The tubercle is the typical lesion of tuberculosis and consists of a partially encapsulated, circumscribed, yellow, firm granulomatous nodule often containing a necrotic and mineralized core with few acid-fast bacilli (Domingo et al. 2014). Tubercles are seen in the organs of the primary site of infection and may progress to larger lesions as the disease becomes chronic (Domingo et al. 2014). Bacilli are more abundant in miliary lesions than in tubercles (Domingo et al. 2014).

Liver

Target. Targetoid lesions (in Portuguese: *lesões em alvo*) are macular or sessile lesions characterized by annular regions of discoloration resulting in a target-like appearance. In the skin, they are often a red or violaceous lesion surrounded by a region of pallor with an outer margin of hyperemia. They can reflect manifestations of dermatophytosis, allergic reactions as well as immune-mediated conditions including erythema multiforme. In addition to the skin, targetoid lesions in the liver of turkeys and broiler breeders are considered characteristic for hepatic histomoniasis (Fig.17) (Abdul-Aziz & Barnes 2018b). *Campylobacter fetus* abortion in sheep similarly results in targetoid lesions in the liver of the lamb fetus where the center represents the necrotic area and the outer rim by inflammatory infiltrate admixed with necrosis (Schlafer & Foster 2015).

Umbilicated. Umbilicated lesions (in Portuguese: *lesões umbilicadas*) are typically dome-shaped with a central depression reflecting intralesional necrosis. The term takes origin from the appearance of the remnant of the umbilicus in neonatal placental mammals. In the domestic species, they are commonly seen as a manifestation of malignant epithelial neoplasia. A well-known example is the cholangiocellular carcinoma (Fig.18), although they can be seen in association with a range of malignant neoplasms including sarcomas.

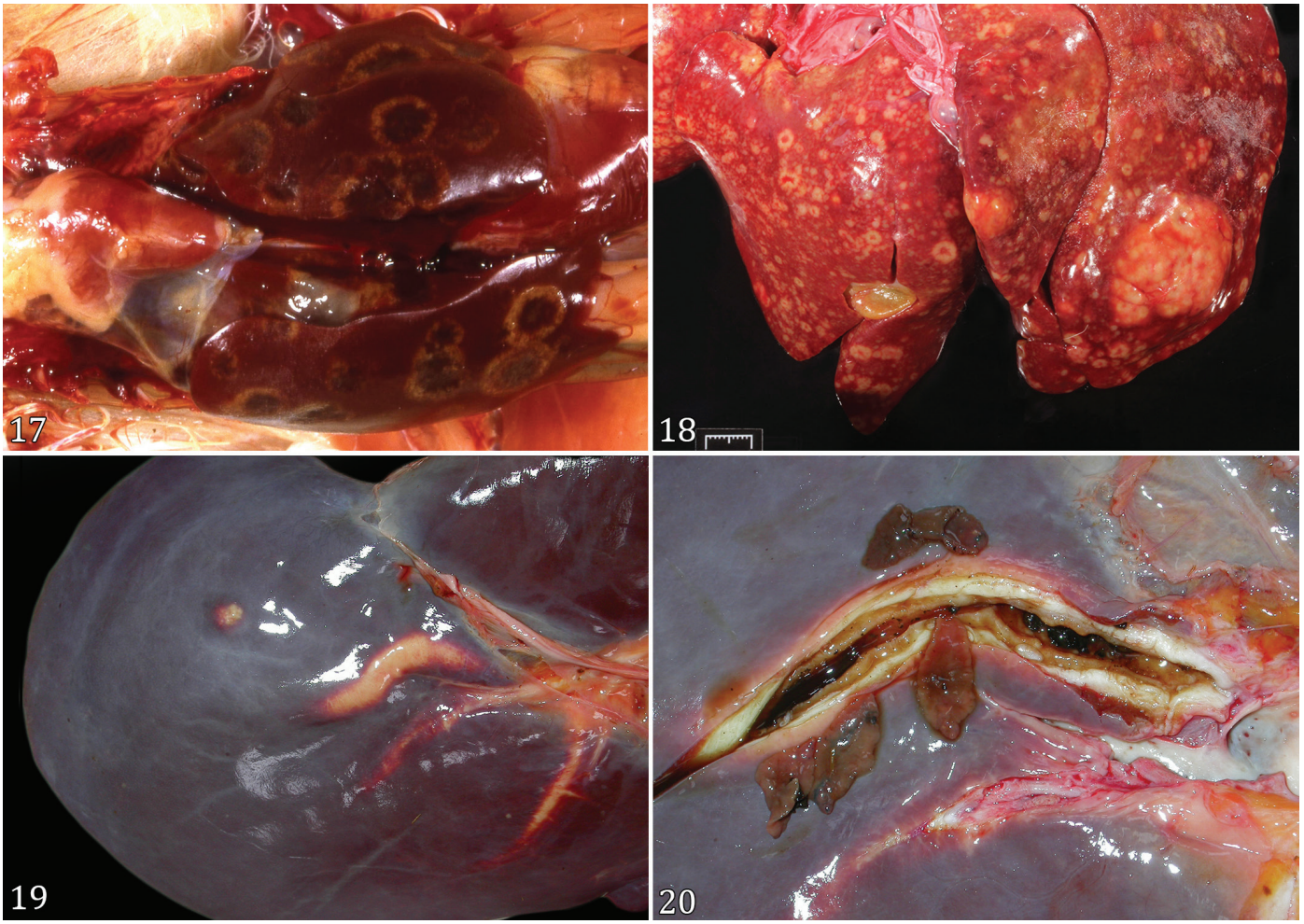

Fig.17-20. (**17**) Multifocal, subacute, necrotizing hepatitis; liver; turkey. Disease: histomoniasis. Shape analogy: Target. In turkeys and chickens, these lesions are characteristic of *Histomonas meleagridis* infection. Photo courtesy: Department of Primary Industries, Victoria, Australia. (**18**) Cholangiocarcinoma; liver; canine. Shape analogy: Umbilicated. The necrotic center of the tumor makes a central depression resembling an umbilicus. Photo courtesy: Dr. Brian Porter, Texas A&M University. (**19**) Chronic hepatic fascioliasis; bovine. Shape analogy: Pipe stem. Enlarged bile ducts are prominent on the visceral surface of the liver. (**20**) Chronic hepatic fascioliasis; bovine. Shape analogy: Pipe stem. Opened bile ducts with thickened, white, and firm wall containing leaf-shaped flukes and dark brown debris (fluke exhaust).

The typical lesion reflects the focal proliferation of neoplastic cells with central collapse as a result of the inability of the neoplasm to maintain adequate blood supply throughout.

Pipe stem. The liver fluke, *Fasciola hepatica,* resides in the bile ducts of cattle, sheep and occasionally other mammalian hosts. This hermaphrodite trematode releases its eggs in bile, which are subsenquently shed in feces. Once in the aquatic environment, a larva (miracidium) is released from the egg and this penetrates the tissues of an aquatic snail, the intermediate host. In the snail, sporocysts, rediae and cercariae develop. Cercariae escape the snail, actively swim, encyst onto the vegetation and become the infective stage, metacercariae. These are ingested by ruminants with the pasture, excyst in the intestine and migrate to the bile ducts (Bowman 2014).

Massive infestation by migrating immature flukes may result in acute disease often resulting in serositis, especially in sheep. Chronic fascioliasis is the most common manifestation and it is characterized by cholangitis induced by the presence of mature flukes. The lesions are seen throughout the liver but are most severe in the left lobe. Enlarged bile ducts are prominent on the visceral surface of the liver as thickened, white, tortuous, mineralized, branching cords, so called "pipe stems" (in Portuguese: *hastes de cachimbo*) (Fig.19 and 20). In cattle, the infection results in the loss of the epithelial lining of the ducts with the associated fibrosis resulting in the duct thickening. The life cycle and lesions of *Fasciola gigantica* are similar to those of *F. hepatica*, but this species is more common in Asia and Africa. In contrast, the American giant liver fluke of deer fluke, *Fascioloides magna,* lives and migrates in the hepatic parenchyma and is not found in the lumen of bile ducts of domestic ruminants, which are dead-end hosts (Cullen & Stalker 2016).

Cardiovascular system

Cauliflower. Valvular endocarditis is characterized by the formation of vegetative growths in the heart's valves that are often compared to cauliflower (in Portuguese: *couve-flor*) (Fig.21). These proliferations are essentially large septic thrombi that are adhered to heart valves. They consist of bacterial colonies, neutrophils, proteins and occasional erythrocytes entrapped in large amounts of fibrin (Robinson & Robinson 2016). Grossly, these nodular masses have a roughened, granular surface with small pits resembling brush-like vegetations. As they enlarge and as they are off-white, the masses are often likened to a cauliflower. Fragments from the surface of these growths can be released into the bloodstream whilst small nodules are continually added as the bacterial colonies continue to proliferate. It is the combination of these two processes that helps gives rise to the irregular vegetative shape.

The common implicated bacteria in valvular endocarditis in animals include *Trueperella pyogenes, Erysipelothrix rhusiopathiae, Streptococcus* spp., *Staphylococcus* spp. and *E. coli* (Robinson & Robinson 2016). Several factors can influence the onset of valvular endocarditis, including recurrent or persistent bacteremia from a distant source, selective bacterial adhesion factors and pre-existing valvular damage such as from micro-trauma due to valvular apposition, turbulent blood flow or a more severe congenital valvular defect (Omobowale et al. 2017).

Saddle thrombus. The thrombus forming at the caudal bifurcation of the aorta into the left and right external iliac arteries is typically Y-shaped. As such, aorto-iliac thrombi are often likened to a saddle (in Portuguese: *trombo em sela*) (Fig.22). The pathogenesis of the saddle thrombus varies in different species accordingly to the primary disease. In cats, it is a common sequela of hypertrophic cardiomyopathy and occurs when a fragment of a thrombus in the dilated left atrium travels in the arterial circulation until it obstructs the aorto-iliac junction (Robinson & Robinson 2016). Although the examination of this area is not part of a routine necropsy, clinical signs such as paresis and cold extremities of the hind limbs should motivate the pathologist to examine the aorto-iliac trifurcation. Aorto-iliac thrombosis is rare in dogs (Lake-Bakaar et al. 2012), cattle (D'Angelo et al. 2006) and horses (Hilton et al. 2008).

Urinary system

Horseshoe kidney. Horseshoe kidney or *ren arcuatus* is a congenital defect representing the renal fusion of the cranial and caudal poles by an isthmus, leading to the characteristic shape of a horseshoe (in Portuguese: *rim em ferradura*) (Fig.23). Embryologically, the kidney arises from two populations: the ureteric bud and the metanephric blastema. In humans, these two structures meet in the upper sacral region (S1-S2) during the fourth week of gestation. Hypotheses for the renal fusion include: abnormalities of growth or ventral flexion within a constricted embryonic pelvis; delayed straightening of the caudal fetus postponing renal ascent to the dorsolumbar position; and alterations in the position of key arteries (e.g., umbilical or common iliac) causing alteration in the path of renal migration. Genetic associations have been investigated (Taghavi et al. 2016).

Morphologically, the majority of horseshoe kidneys are usually fused at the lower pole by a large isthmus (Taghavi et al. 2016). Because renal parenchyma and function are normal, horseshoe kidneys remain undetected during life and are an incidental finding at necropsy.

Wedge-shaped infarcts. Kidneys are susceptible to infarction due to the disposition of their arterial vasculature and high circulating blood volume (Breshears & Confer 2017). Renal infarcts are areas of localized coagulative necrosis produced by embolic or thrombotic occlusion of the renal artery or its branches (Breshears & Confer 2017). In the kidney, infarcts are usually triangular or wedge-shaped (In Portuguese: *infarto em cunha*) in a cross section, with the base against the cortical surface and the apex pointing toward the medulla. In rare occasions, emboli may occlude the renal artery and cause total or subtotal infarction of the kidney (Breshears & Confer 2017). Occasionally, emboli occlude the arcuate arteries, with triangular or wedge-shaped areas of infarction involving both the renal cortex and medulla (Fig.24) (Cianciolo & Mohr 2016). Most commonly, emboli obstruct smaller vessels (e.g., interlobular arteries), causing triangular or wedge infarcts limited to the renal cortex (Cianciolo & Mohr 2016). Acute infarcts are swollen, congested, without a sharp line demarcation from the adjacent normal tissue (Cianciolo & Mohr 2016). Within 2-3 days, the infarcted area becomes white and is outlined by a thin layer of leukocytes (Cianciolo & Mohr 2016). Within weeks, the area of coagulative necrosis is progressively replaced by fibrous tissue and becomes a wedge-shaped, pale-white, depressed, firm scar (Cianciolo & Mohr 2016). In addition to infarcts, septic thrombi may also produce abscesses (Cianciolo & Mohr 2016).

Botryoid rhabdomyosarcoma of the urinary bladder. Rhabdomyosarcoma, a malignant tumor of striated muscle, has a characteristic gross aspect when arising in the urinary bladder and urethra. Here they often form multilobular masses resembling a bunch of grapes hence are referred to as botryoid (in Portuguese: *rabdomiosarcoma botrioide*) (Caserto 2013). The exact cell of origin in the urinary bladder is unknown, but skeletal muscle can be found in the urethra and in the fundus of the urinary bladder (Meuten & Meuten 2017). Botryoid rhabdomyosarcomas are uncommon in animals and affect more frequently young dogs. Females, Basset hounds and large breed dogs are overrepresented (Meuten & Meuten 2017). Occasionally, botryoid rhabdomyosarcomas in the urinary bladder may be associated with hypertrophic osteopathy, with resolution of the bone lesions after resection of the tumor, although the mechanism is not known (Meuten & Meuten 2017).

Musculoskeletal system

Lumpy jaw. Mandibular actinomycosis is a pyogranulomatous osteomyelitis, primarily of cattle. The osteomyelitis involvement of the jaw (the most common site of the lesion) takes an aspect of an irregularly contoured swelling colloquially referred to as lumpy jaw (Fig.25) (Wilson 2005, Craig et al. 2016). This translates literally into Portuguese as "*queixada encaroçada*", although this particular phrasing is not used in Brazil to describe this entity. The preferred term is in Portuguese is "*actinomicose*".

It is caused by a gram-positive bacterium, *Actinomyces bovis* (Craig et al. 2016), that occurs as commensal in the oral cavity. Occasionally, as a result of mucosal damage, *A. bovis* penetrates the tissues causing focal osteomyelitis in the mandible (Tessele et al. 2014), but less commonly, elsewhere. The affected tissue, usually the mandible, becomes thickened as a result of multiple pyogranulomas (Grist 2008). Usually, the lesion develops fistulae, and pus exudes through the fistulae to the outside (Fig.25). The lumpy thickening of the bone gives the lesion the appearance of a honeycomb (Fig.26). Occasional infections occur in other species such as pigs, deer, dogs, sheep, goats and horses (Craig et al. 2016). It has also been reported in Australian macropods although here *Fusobacterium necrophorum* is the most common

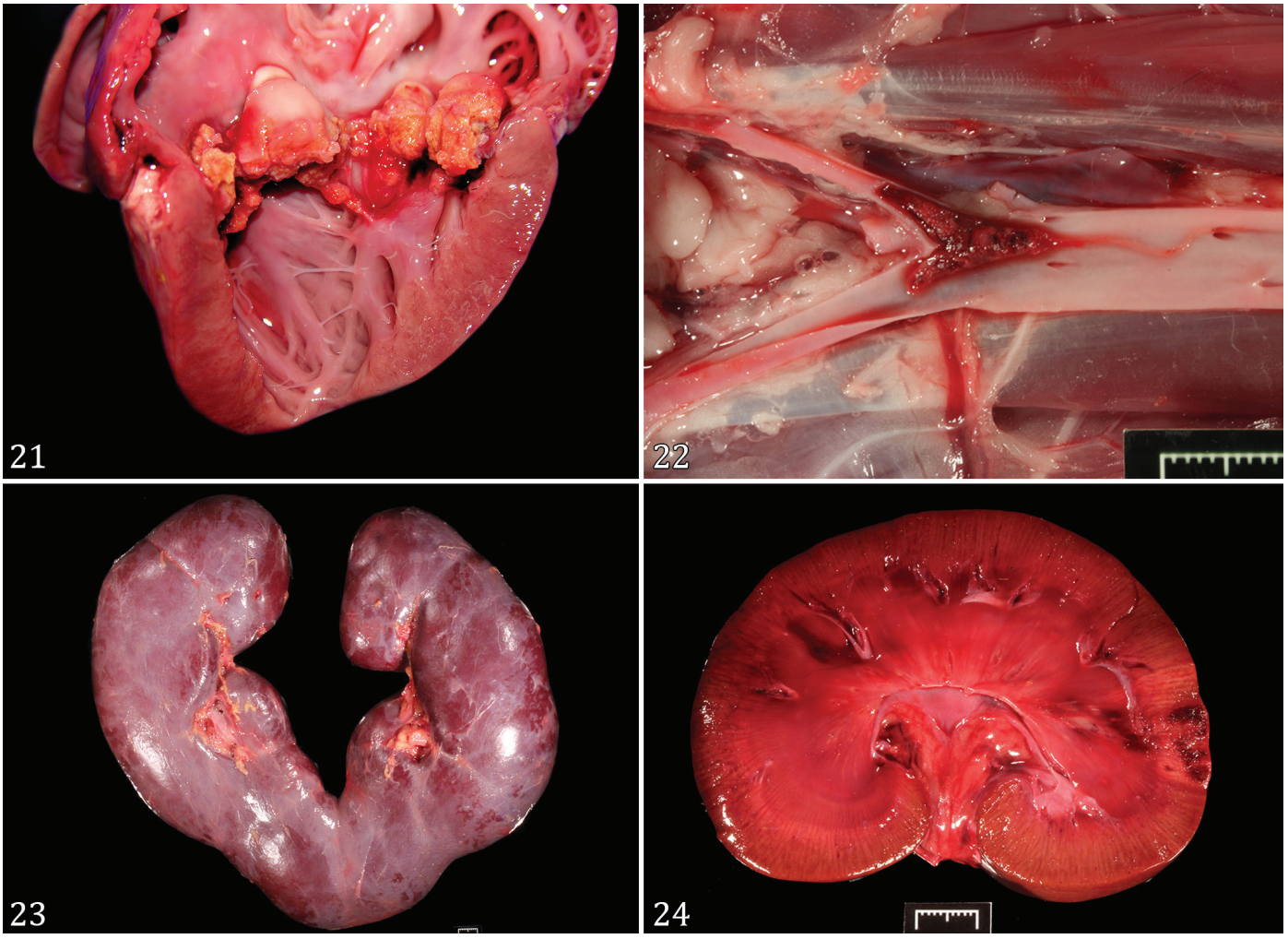

Fig.21-24. (**21**) Marked, acute, fibrinosuppurative, vegetative endocarditis; mitral valve; swine. Shape analogy: Cauliflower. Large, pale, vegetative growths on the mitral valve secondary to bacterial infection resemble a cauliflower. (**22**) Locally extensive, acute, aorto-iliac thrombosis secondary to hypertrophic cardiomyopathy; feline. Shape analogy: Saddle thrombus. The lumen of the aortoiliac junction is occluded by a Y-shaped thrombus. (**23**) Horseshoe kidney; equine. Shape analogy: Horseshoe. The caudal poles of the kidneys are fused by an isthmus. (**24**) Focally extensive renal infarct; canine. Shape analogy: Wedge-shaped. Affecting both the renal cortex and medulla is a focally extensive, wedge-shaped, red area of ischemic necrosis surrounded by a pale rim halo.

bacterial isolate (Brookins et al. 2008). In humans, the injury is caused by *A. israeli* (Jones et al. 1997).

MICROSCOPIC FINDINGS

Integument or skin and appendages

Club-shaped. Structures consisting of radially arranged brightly eosinophilic, club-shaped (in Portuguese: *em forma de clava* or *claviforme*) (Fig.27) are known by the eponym of Splendore-Hoeppli (S-H) phenomenon. The eosinophilic clubs typically radiate around the inciting organism forming star-like or asteroid configurations (Lurie 1971) and are commonly surrounded by variable numbers of neutrophils, which are surrounded by epithelioid macrophages.

The S-H phenomenon is a reaction to microorganisms such as bacteria, fungi, larger parasites or biologically inert substances. It was originally observed in cases of sporotrichosis (*S. asteroides*) by Splendore (Splendore 1908) and in cases of schistosomiasis by Hoeppli (1932) and was attributed to the deposition of antigen-antibody complexes, glycoproteins, and debris from host inflammatory cells, including fibrin (Lurie 1971). Microscopically, the S-H reaction appears as a strongly eosinophilic, radiating, amorphous material in the center or around the causative agent (Gopinath 2018). However, there is a dispute over the exact nature of the Splendore-Hoeppli reaction. Some have suggested it to represent glycoproteins, lipid and calcium derived from host leukocytes, as well as eosinophil major basic protein (Hussein 2008). As such, it would seem appropriate for it to be considered a localized immunological host reaction with a composition likely to vary, representing a unique balance between organism, its virulence and the host response.

Flame figures. Flame figures (in Portuguese: *figuras em chama* or *figuras brilhantes*) are represented by a focal area in the dermis where collagen fibers are surrounded by eosinophils and covered by eosinophil granules as well as an amorphous eosinophilic material (Fig.28) (Gross et al. 2005c). This material is variable in shape, from annular to oval, to a radiating configuration resembling the spokes of a wheel (starburst appearance) (Scott & Miller 2010). In chronic cases, these areas are often surrounded by a mantle of palisading macrophages which are believed to be a response to the material liberated from the eosinophils (Gross et al. 2005c, Fairley 1991). The histological appearance of the flame figures reflects the edema between collagen fibrils, clusters of free eosinophil granules and eosinophil debris (Bardagí et al. 2003). Major basic protein from eosinophil granules is a component of the material which accumulates in the flame figures (Peters et al. 1983, Wouters et al. 2015).

Flame figures were first described in a group of human patients suffering from granulomatous dermatitis with eosinophilia (Wells 1971). These structures have since been noted in a range of eosinophil-rich dermatitides of humans and animals. Most commonly reported in cats and horses in association with the eosinophilic granuloma, they can also be seen in a range of species with a spectrum of skin diseases in which there is a significant contribution by eosinophils (Fernandez et al. 2000). These include the spectrum of hypersensitivity reactions to agents such as arthropods, food and environmental allergens, as well as even viral, bacterial or fungal infections. They can also be noted in association with equine and canine mast cell tumors.

Witches feet. Follicular dysplasias are a group of skin diseases in dogs with varying clinical and microscopic features resulting from the abnormal growth and development of hair (Gross et al. 2005a). Microscopic changes include some degree of atrophy of the hair follicles along with marked infundibular hyperkeratosis with the formation of comedones and keratin that extends into the opening of secondary follicles (Laffort-Dassot et al. 2002). This can make the hair follicles resemble a broad, malformed foot (primary follicle expanded by keratin) with

Fig.25-26. (**25**) Marked, locally extensive, pyogranulomatous osteomyelitis; bovine. Etiology: *Actinomyces bovis*. Shape analogy: Lumpy jaw. A large, ulcerated hard mass expands the left mandible. (**26**) Marked, locally extensive, pyogranulomatous osteomyelitis; mandible, bovine. Shape analogy: Lumpy jaw. The affected bone was macerated, and the honeycomb aspect can be appreciated. The "holes" were once filled by pyogranulomatous inflammation that protruded over the borders of the holes, giving the jaw a lumpy look.

irregular toes and sharp nails (expanded secondary follicles) (Miller & Dunstan 1993) resembling witches feet (in Portuguese: *pés de bruxa*) (Fig.29). Follicular dysplasias are typically breed-associated conditions often with a demonstrable hereditary basis. Examples include a range of breed-specific conditions as well as cyclical flank alopecia, color dilution alopecia and black hair follicular dysplasia (Gross et al. 2005a).

Railroad tracks. *Dermatophilus congolensis* is a gram-positive, actinomycete bacteria that causes exudative dermatitis in a wide host range, but it is more common in ruminants (Mauldin & Peters-Kennedy 2016). Trauma to the skin and prolonged moisture are determinant factors involved in the pathogenesis of dermatophilosis (Mauldin & Peters-Kennedy 2016). Chronic lesions are composed of alternating layers of parakeratotic and orthokeratotic keratin and degenerate neutrophils (Mauldin & Peters-Kennedy 2016). On cytology and histopathology (Fig.30), cocci of *D. congolensis* are arranged forming parallel branching filaments called railroad tracks (in Portuguese: *trilhos de trem*) (Mauldin & Peters-Kennedy 2016). Under appropriate wet conditions, cocci are activated to become motile, infective zoospores that can be transmitted to other animals and occasionally humans (Towersey et al. 1993, Mauldin & Peters-Kennedy 2016).

Owl's eye nuclei. On occasion, cell nuclei can be seen to take on an owl's eye appearance (in Portuguese: *núcleo em olho de coruja*). These are characterized by a large nucleus bearing either a prominent nucleolus (Fig.31) or a large intranuclear viral inclusion. In addition, there are accompanying varying degrees of perinucleolar clearing and/or peripheral margination of chromatin. This form of nuclei is seen in a relatively limited number of circumstances including cytomegalovirus infection (Cowdry type A inclusions) (Mattes et al. 2000), as a feature of Reed-Sternberg cells seen with T-cell-rich B-cell lymphoma/Hodgkin-like lymphoma (Valli et al. 2002). Owl's eye nuclei are associated with marked nuclear atypia with anaplastic malignant neoplasia including malignant melanoma and neoplasms of muscle origin (Cooper & Valentine 2017).

Keratin pearls. The keratin pearl (in Portuguese: *pérola de queratina*) is a hallmark histological feature of the well-differentiated squamous cell carcinoma and it can on occasion be seen at sites of marked epidermal hyperplasia. Keratin pearls typically form within the infiltrating nests and cords of neoplastic squamous epithelium characteristic of squamous cell carcinomas. They are composed of a central laminated mass of keratin surrounded by concentric layers of atypical squamous cells (Fig.32). Their formation is similar to a pearl within the oyster in which the so-called pearl-sac epithelium secretes thin layers of nacreous matter around a small nucleus (Sato et al. 2013).

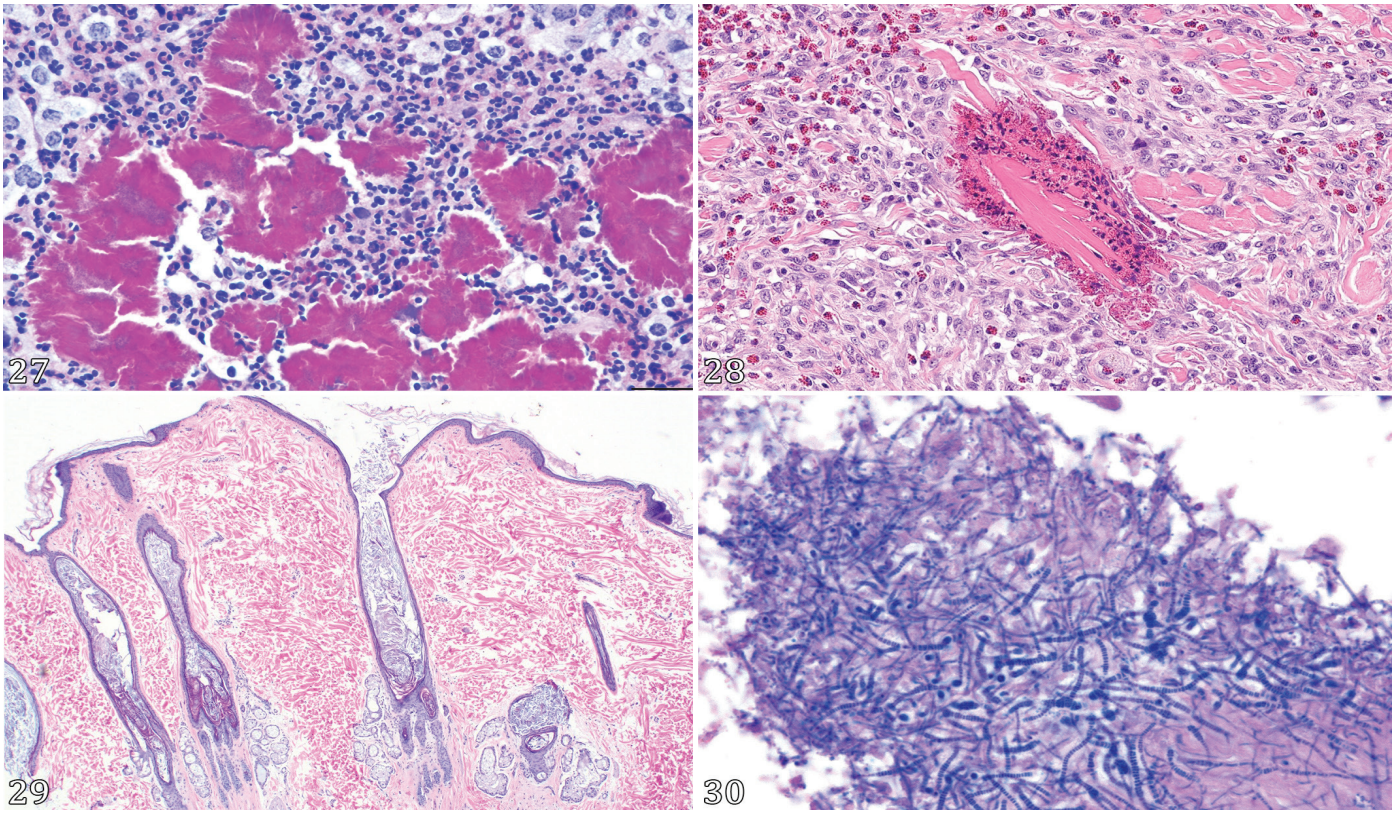

Fig.27-30. (**27**) Chronic, pyogranulomatous dermatitis with club-shaped Splendore-Hoeppli material, muzzle; bovine. Shape analogy: Club-shaped. HE, obj.20x. (**28**) Chronic, eosinophilic and granulomatous dermatitis; haired skin; equine. Disease: habronemiasis. Shape analogy: Flame figure. A focal aggregate of brightly eosinophilic collagen fibers is covered and surrounded by eosinophils. HE, obj.20x. (**29**) Follicular dysplasia; haired skin; canine. Disease: cyclical flank alopecia. Shape analogy: Witches feet. Atrophy of the hair follicles along with marked infundibular hyperkeratosis and the extension of keratin into the opening of secondary follicles resemble a broad, malformed foot with irregular toes and sharp nails. HE, obj.4x. Photo courtesy: Dr. Dominique J. Wiener, Texas A&M University. (**30**) Marked, diffuse parakeratotic and neutrophilic dermatitis with abundant filamentous bacteria; haired skin; bovine. Disease: dermatophilosis. Shape analogy: Railroad track. Cocci of *Dermatophilus congolensis* are arranged forming parallel branching filaments. HE, obj.40x

The squamous cell carcinoma (SCC) is the most common malignant skin tumor of all domestic species, including the chicken (Goldschmidt & Goldschmidt 2017). Their occurrence is often associated with excessive ultraviolet irradiation from sun exposure. In cattle, sheep and goats the vulva is a common primary site although other sparsely haired regions such as the pinna, eyelids, conjunctiva and mucocutaneous junctions can be affected. Breeds such as the Hereford and Simmental, which often lack circumocular pigmentation, have an increased incidence of ocular SCC. In horses, sparsely haired regions are again most vulnerable with the eyelids and conjunctiva as well as the penis and prepuce being common locations. In dogs, non-pigmented areas in short-coated breeds are commonly affected. As such, frequent locations in dogs include the ventral abdomen, medial surfaces of the limbs as well as the perineum and these are often seen in dogs who like to sunbathe. The nail bed is also the origin of a subungual SCC in dogs. In cats the pinna, nasal planum and eyelids are by far the most common sites again with non-pigmented regions being most vulnerable. Cutaneous SCC has been associated with papillomavirus infection such as *Ovis aries* papillomavirus 3 in sheep (Vitiello et al. 2017) and *Equus caballus* papillomavirus 2 in penile SCC in horses (Lange et al. 2012).

In addition to cutaneous and mucocutaneous tumors, SCC is also a very common neoplasm of the upper alimentary tract. It is the most common oral malignancy in production animal species, horses and cats as well as being the second most common oral malignancy in dogs (Munday et al. 2017). In dogs, tumors arising from the tonsillar epithelium often display the most aggressive behavior of the oral SCC. In cattle, a clear causal association has been made between the ingestion of bracken fern (*Pteridium arachnoideum*) and the occurrence of SCC in the oral cavity, esophagus and rumen as well as with lower urinary tract neoplasia and enzootic hematuria (Döbereiner et al. 1967, Jarrett et al. 1978, Souto et al. 2006, Lucena et al. 2011, Masuda et al. 2011). Whilst it seems the oncogenic agents in bracken fern can induce neoplasia independently (Campo et al. 1985, Souto et al. 2006), bovine papillomavirus 4 (BPV-4) is also a well-known cocarcinogen in these tumors with malignant transformation occurring within the virally-induced papillomas in the upper alimentary tract (Jarrett et al. 1978, Campo et al. 1980, Campo 1997, Souto et al. 2006).

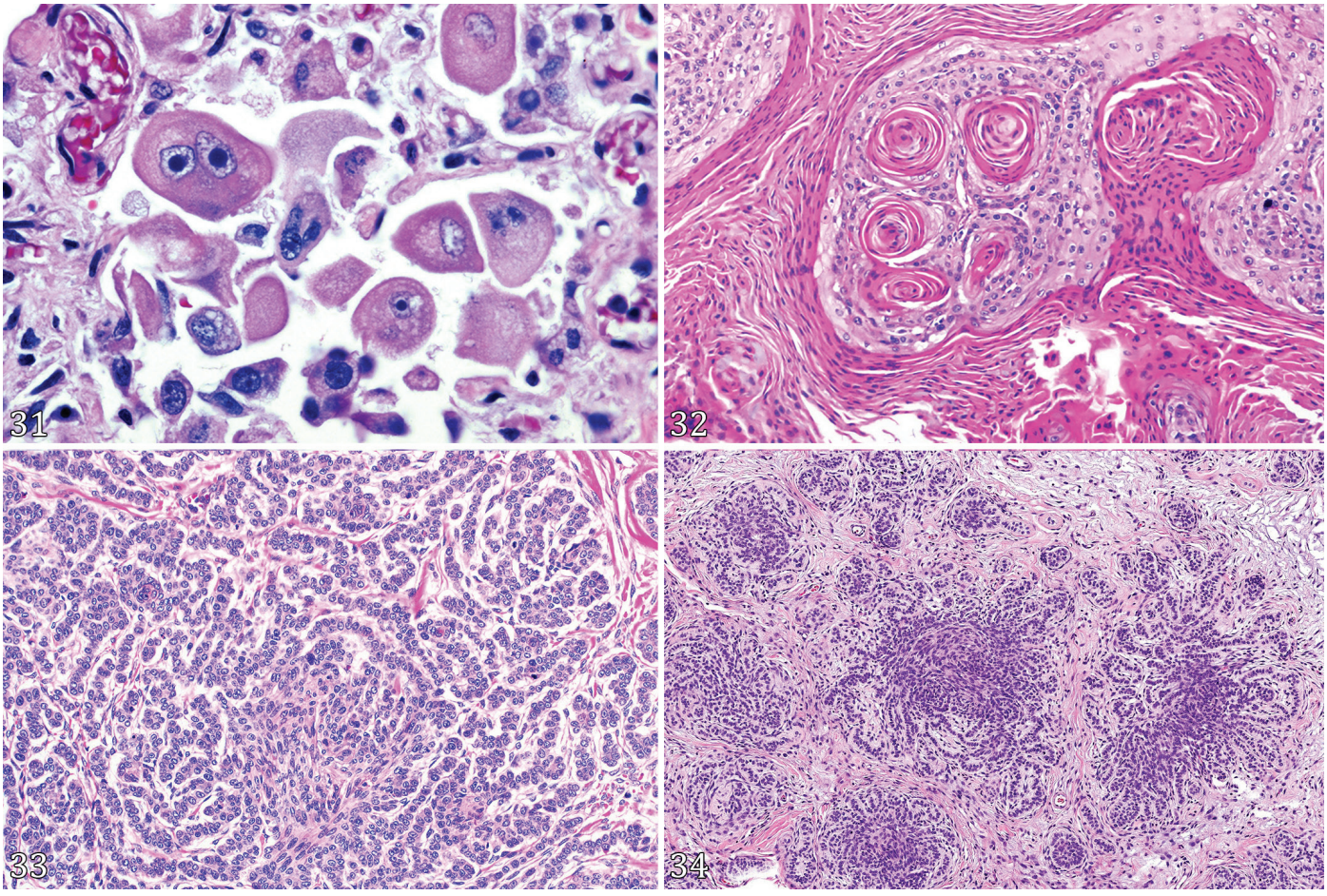

Fig.31-34. (**31**) Anaplastic pulmonary carcinoma; lung; canine. Shape analogy: Owl's eye nuclei. The neoplastic cells often have large, atypical nuclei bearing a prominent nucleolus and some perinucleolar clearing. The atypical nuclei resemble an owl's eye with the nucleolus representing the pupil. HE, obj.40x. (**32**) Squamous cell carcinoma; haired skin; equine. Shape analogy: Keratin pearl. Central laminated masses of keratin are surrounded by concentric layers of neoplastic squamous epithelial cells. HE, obj.20x. (**33**) Trichoblastoma, ribbon type; haired skin; canine. Shape analogy: Ribbons. The cords of cells resemble bundles of ribbons or streamers. HE, obj.10x. (**34**) Trichoblastoma; medusoid type; haired skin; canine. Shape analogy: Medusa head. The ribbons of cells radiating out from a central point resemble the head of the well-known monster of Greek mythology. HE, obj.4x.

Ribbon or medusoid trichoblastoma. Trichoblastomas are derived from the primitive hair germ of embryonal follicular development (Wiener 2021). These slow-growing, benign tumors occur most commonly in the dog and cat with a predilection for the head and neck region (Goldschmidt & Goldschmidt 2017). Histologically, five subtypes are described: ribbon, spindle, granular cell, trabecular and with outer root sheath differentiation. In all of the subtypes, small clusters of mesenchymal cells may be seen in the stroma close to the epithelial neoplastic cells, resembling dermal papillae (follicular papillary mesenchymal bodies) (Wiener 2021). Histologically, trichoblastomas are composed of small, basaloid keratinocytes arranged in branching and radiating columns, usually 2-3 cells in width (ribbon trichoblastoma) (in Portuguese: *tricoblastoma em fita*) (Fig.33). Nests of ribbons of cells can radiate out from a central point, giving the impression of a medusoid arrangement (medusoid trichoblastoma) (in Portuguese: *tricoblastoma medusoide*), as the snake-like structures of Medusa's head (Fig.34) (Goldschmidt & Goldschmidt 2017).

Digestive system

Ink drop structures. Evaluation of architectural arrangements is a useful tool for recognizing epithelial cells that are of odontogenic origin. Odontogenic epithelial cells can be arranged in thin plexiform ribbons, broad anastomosing trabeculae, round follicles or ink drop structures. Ink drop (in Portuguese: *gota de tinta*) structures are unique to odontogenic epithelium and these formations are commonly seen within odontogenic tumors (Fig.35). Some even consider ink drop arrangements to be pathognomic for odontogenic epithelium. Ink drop structures are less commonly referred to as medusoid configurations. They are likened to the shape formed when ink is dropped onto a solid surface. Within histologic ink drop structures, the epithelial cells also tend to exhibit most or all of the cardinal features of odontogenic epithelium, including palisading of the basilar epithelium, antibasilar nuclear polarization of palisading cells, basilar clear cytoplasmic zone of palisading cells and central cells reminiscent of stellate reticulum (Murphy et al. 2020).

Volcano ulcers. *Clostridioides difficile* causes diarrhea and colitis in humans and several animal species, including horses, pigs, rabbits, hares, primates, dogs, cats, ostriches and prairie dogs (Uzal et al. 2016). The disease most commonly develops after antibiotic therapy or hospitalization (Baverud et al. 1998; Madewell et al. 1995). *C. difficile* produces two exotoxins, toxin A (enterotoxin) and toxin B (cytotoxin and enterotoxin) that can be detected in gut content or feces in order to confirm the diagnosis (Diab et al. 2013). These toxins affect the cytoskeleton and tight junctions of enterocytes, activate intestinal secretion and cause release of proinflammatory cytokines attracting neutrophils (Keel & Songer 2006). Therefore, the intestinal content of affected animals is excessively fluid, with focal or diffuse small intestinal and/or colonic epithelial necrosis (Uzal et al. 2016). Histologically, the exudation of neutrophils and fibrin into the intestinal lumen through the ulcerated mucosa is referred as a "volcano ulcer" (in Portuguese: *úlcera em vulcão*) (Uzal et al. 2016) due to its similarity with volcanic eruptions.

Signet ring cells. Signet ring is a finger ring with a signet or seal set into the ring forming an eccentric, thickened region to the ring circumference. In pathology, the term signet ring cell (in Portuguese: *célula em anel de sinete*) is used to describe cells with an eccentric nucleus displaced by a large cytoplasmic vacuole (Fig.36). In veterinary pathology, signet ring cells are a diagnostic feature of urothelial carcinomas (Meuten & Meuten 2017). In canine gastric and intestinal adenocarcinomas, the intracytoplasmic vacuole contains mucin. Signet-ring variants has been described in anal sac gland carcinomas, liposarcoma of bone and melanoma.

Liver

Pick-up sticks. Tyzzer's disease is caused by *Clostridium piliforme*, a spore-forming, gram-negative bacterium (Barthold et al. 2016). The disease affects various mammal species including rodents, rabbits, horses and cats (Gelberg 2017). The main target organ is the liver, but necrotizing enteritis and myocarditis can also occur (Barthold et al. 2016). Bacilli of *C. piliforme* are observed within the cell (Fig.37), lying in a unique criss-crossed arrangement which has been described

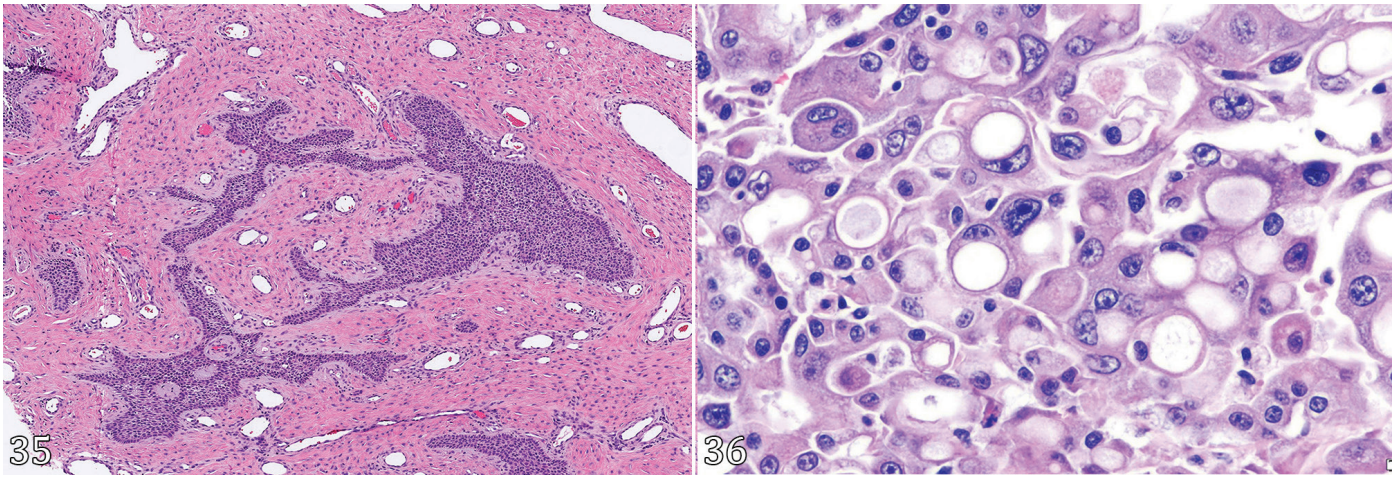

Fig. 35-36. (**35**) Ameloblastoma; tooth; canine. Shape analogy: Ink drop structures are characteristic of odontogenic epithelium origin. HE, obj.4x. (**36**) Urothelial carcinoma; urinary bladder; canine. Shape analogy: Signet ring cells. These cells are a feature of urothelial carcinomas. HE, obj.40x.

as oriental letters or pick-up sticks (Fig.38) (in Portuguese: *letras orientais* or *pega varetas*) around the necrotic cells (Gelberg 2017).

Maltese crosses. In humans and animals with porphyria disorders, a defect in hemoglobin metabolism results in accumulation of porphyrin pigments in the blood and certain tissues (Lecha et al. 2009). In veterinary medicine, congenital erythropoietic porphyria is perhaps the best-known example and is a well-described, inherited disorder of various cattle, namely Limousin and Blonde d'Aquitaine breeds. Porphyria disorders have also been described in pigs, chickens, cats and as an acquired disease in a few dogs (Cullen et al. 2016, Ueda et al. 2005). Histologically, porphyrin pigment is seen as orange-brown, spherical pigment deposited within hepatocytes and bile canaliculi (Fig.39). Under polarized light, this pigment has red crystalline birefringence with characteristic Maltese cross-like shapes (Fig.40) (in Portuguese: *cruz de Malta*). The Maltese cross is a historical symbol made famous by the Knights Hospitaller, also known as the Knights of Malta. It is formed by four symmetrical triangle or cone shapes arranged perpendicularly with the tips converging on a center point. The reason for this unique pattern of birefringence in porphyrin pigment relates to the polymer structure of the crystalline pigment and physical properties affecting light transmittance, a discussion beyond the scope of this paper.

Urinary system

Sheaves of wheat and prisms. Abundant calcium oxalate crystals can be observed in the renal tubules and around cerebral vessels of dogs and cats intoxicated with ethylene glycol, an antifreeze solution (Smith et al. 1990, Cianciolo & Mohr 2016). The crystals are light yellow, are highlighted by polarized light and arranged in fashion which resemble sheaves of wheat or prisms (Fig.41 and 42) (in Portuguese: *feixes de trigo* or *prismas*) (Cianciolo & Mohr 2016). Associated lesions are more severe in the renal proximal tubules and include tubular degeneration, necrosis and regeneration (Cianciolo & Mohr 2016). In grazing ruminants, plants are the usual source of oxalates, including *Halogeton glomeratus, Sarcobatus vermiculatus, Oxalis cernua* and *Rumex* spp. (Cianciolo & Mohr

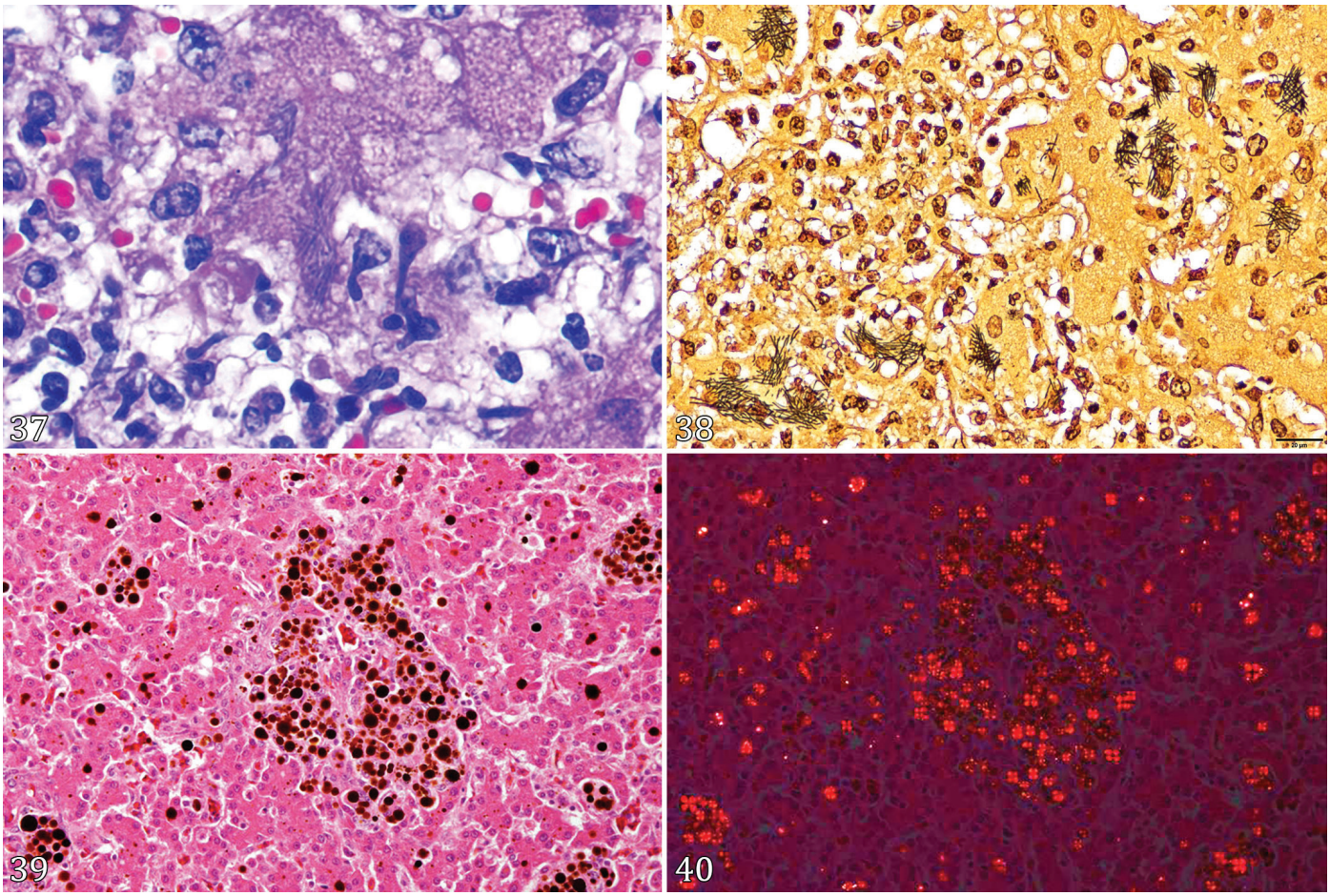

Fig.37-40. (**37**) Multifocal, random, subacute, necrosuppurative hepatitis with hepatocellular bacilli; liver; equine. Disease: Tyzzer's disease. Shape analogy: Pick-up sticks. HE, obj.40x. (**38**) Multifocal, random, subacute, necrosuppurative hepatitis with hepatocellular bacilli; liver; equine; Cause: *Clostridium piliforme*. Shape analogy: Pick-up sticks. Bacilli lay in a criss-crossed arrangement within the cytoplasm of hepatocytes, better visualized with a silver stain. Steiner stain, obj.20x. (**39**) Protoporphyrin accumulation; liver; chicken. Shape analogy: Maltese cross. Rounded, dark brown bodies within hepatocytes and bile ducts. HE, obj.20x. Photo courtesy: Dr. Monique França, The University of Georgia. (**40**) Protoporphyrin accumulation; liver; chicken. Shape analogy: Maltese cross. Under polarization, the pigmented round structures in Figure 39 display a characteristic bright-orange aspect with a centrally-located Maltese cross. HE, obj.20x. Photo courtesy: Dr. Monique França, The University of Georgia.

2016). Fungal species like *Aspergillus nig*er and *A. flavus* can synthesize oxalic acid on forage (Cianciolo & Mohr 2016) or in sites of *Aspergillus* spp. infection, especially in the respiratory tract, resulting in precipitation of calcium oxalate crystals (Payne et al. 2017).

Pinwheel crystals. Characteristic renal tubular crystals have been reported in dogs, cats and pigs that ingested commercial food contaminated with melamine and cyanuric acid (Brown et al. 2007, Nilubol et al. 2009, Yhee et al. 2009). When combined, these chemicals form insoluble crystals that obstruct and damage the renal distal tubules and collecting ducts, leading to renal failure (Puschner et al. 2007). The crystals are 10-40µm, polarizable, light green to brown with two or more concentric circles with radiating striations resembling spokes (Fig.43) and hence to comparison to pinwheels (in Portuguese: *catavento*) (Yhee et al. 2009).

Brick inclusions. Brick inclusions (in Portuguese: *inclusões retangulares semelhantes a tijolos*) are intranuclear, non-specific inclusions that are found commonly in aged dogs. These inclusions are typically brightly eosinophilic, crystalline and rectangular/block shaped (Fig.44). They are most commonly found in the kidney, especially in proximal tubular epithelial cells, and in the liver. Brick inclusions have no clinical significance and are considered incidental findings. Their cause is unknown. It is important for pathologists to be able to recognize brick inclusions and to be able to differentiate them from viral inclusion bodies and inclusion bodies caused by lead toxicosis (Cianciolo & Mohr 2016, Cullen & Stalker 2016).

Nervous system

Acicular clefts. Acicular means needle-shaped or slender leaf-shaped (in Portuguese: *acicular*). It is used most commonly used in pathology to describe the shape of the clefts left behind in tissues after cholesterol crystals have been removed during tissue processing. Cholesterol is a significant component of cellular membranes and, as such, any lesion in which there is a significant degree of cellular degeneration can leave behind collections of cholesterol crystals. In tissue sections the resultant clefts often palisade, forming picket fence type

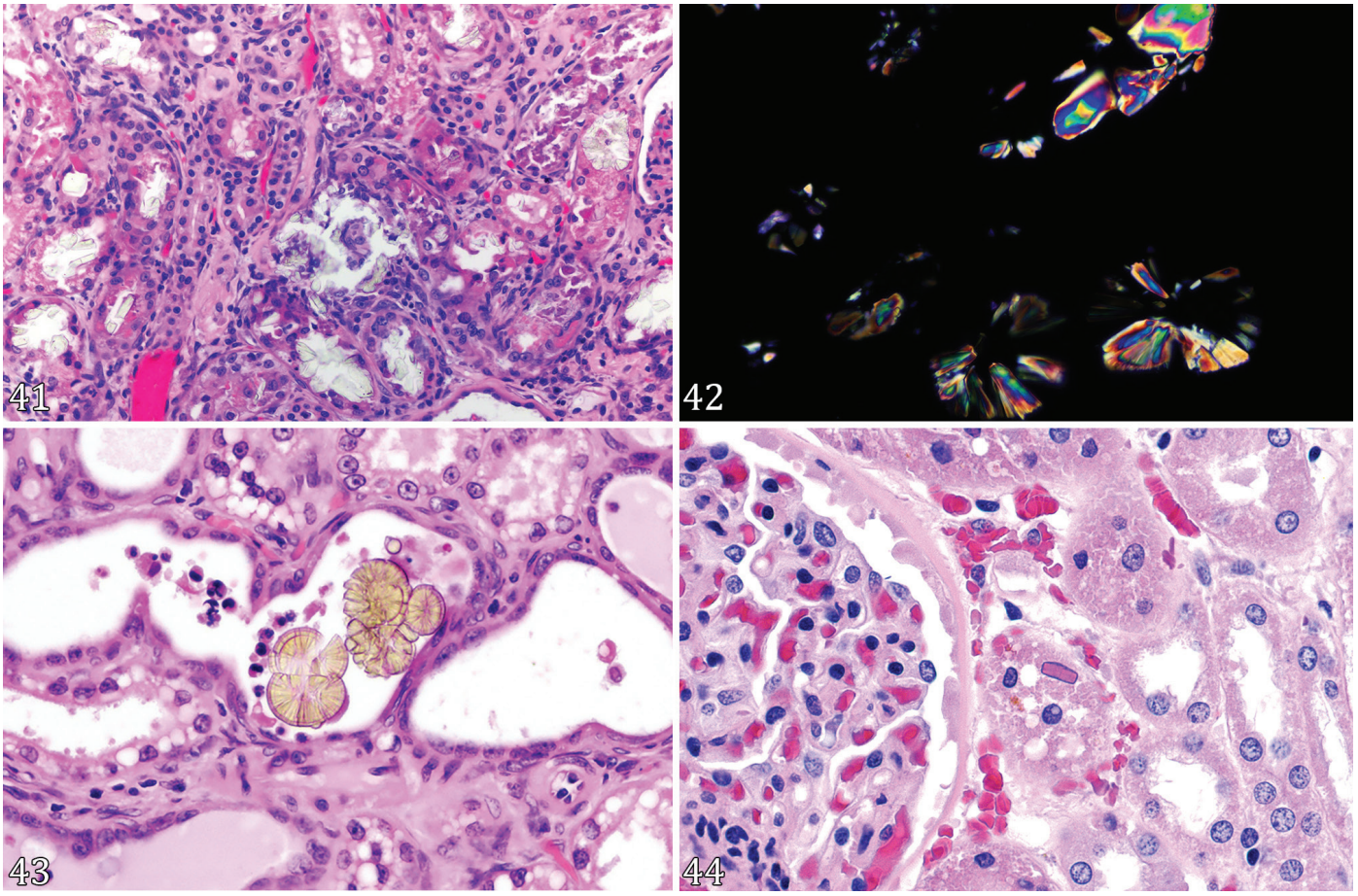

Fig.41-44. (**41**) Moderate, multifocal, acute tubular degeneration and necrosis with intratubular crystals; kidney; canine. Cause: ethylene glycol toxicosis. Shape analogy: Sheaves of wheat. The renal tubules contain refractile oxalate crystals similar to sheaves of wheat. HE, obj.20x. (**42**) Oxalate crystals; kidney; canine. Cause: ethylene glycol toxicosis. Shape analogy: Prisms (in Portuguese: prismas). Under polarized light, the crystals are similar to prisms. (**43**) Marked, multifocal tubular degeneration and attenuation with intratubular crystals; kidney; canine. Cause: melamine and cyanuric acid toxicosis. Shape analogy: Pinwheel crystals. The distal tubules contain green-brown, circular crystals with radiating spokes, cellular debris and neutrophils. HE, obj.40x. (**44**) Acidophilic, rectangular, intranuclear inclusions; kidney; canine. Shape analogy: Brick inclusions. These are a common incidental finding in the proximal renal tubules and hepatocytes of old dogs. HE, obj.40x.

arrangements. These clefts can be seen in benign cystic lesions, any neoplasm, chronic inflammatory lesions, atherosclerotic plaques, xanthomatous lesions as well as cholesteatomas/cholesterol granulomas in horses (Fig.45). These clefts often have an associated infiltrate of macrophages. Eosinophilic acicular crystals can also be seen in the lung of laboratory mice, especially 129 strains. These occur in a condition known as eosinophilic crystalline pneumonia (also referred to as acidophilic macrophage pneumonia) (Barthold et al. 2016).

Serpentine or serpiginous tracks. High-grade astrocytomas and oligodendrogliomas often contain intratumoral necrosis arranged in serpiginous tracks (in Portuguese: *necrose em trajetos serpiginosos*) where neoplastic cells can palisade around necrotic areas (Fig.46) (Higgins et al. 2017, Koehler et al. 2018). Gliomas account for 30% of the primary nervous system tumors. Brachycephalic breeds such as Boxers, Bulldogs and Boston terriers have about 23 times higher incidence to develop gliomas than other breeds of dogs (Higgins et al. 2017).

Glomeruloid vascular proliferation. Glomeruloid vascular proliferation (in Portuguese: *proliferação vascular glomeruloide*) are newly sprouted vessels arranged in tufted aggregates resembling renal glomeruli. Microvascular proliferation is a hallmark of high-grade oligodendrogliomas and astrocytomas with robust foci of glomeruloid vessels (Fig.47) forming a rim along the periphery of the tumor, and often noted in zones surrounding pseudopalisading necrosis. The presence of microvascular proliferation and necrosis are the most reliable features to differentiate a low-grade from a high-grade astrocytoma or oligodendroglioma (Koehler et al. 2018).

Rosettes. Rosettes (in Portuguese: *rosetas*) are comprised of a halo, flower-like, or spoke-wheel arrangement of cells surrounding a central space and are common features of neural tumors (Wippold & Perry 2006). Several types of rosettes are recognized in the literature. A Homer-Wright rosette contains a halo of neuroblastic cells surrounding a lumen filled with their processes and occurs in medulloblastomas and other primitive neuroectodermal tumors (Wippold & Perry 2006).

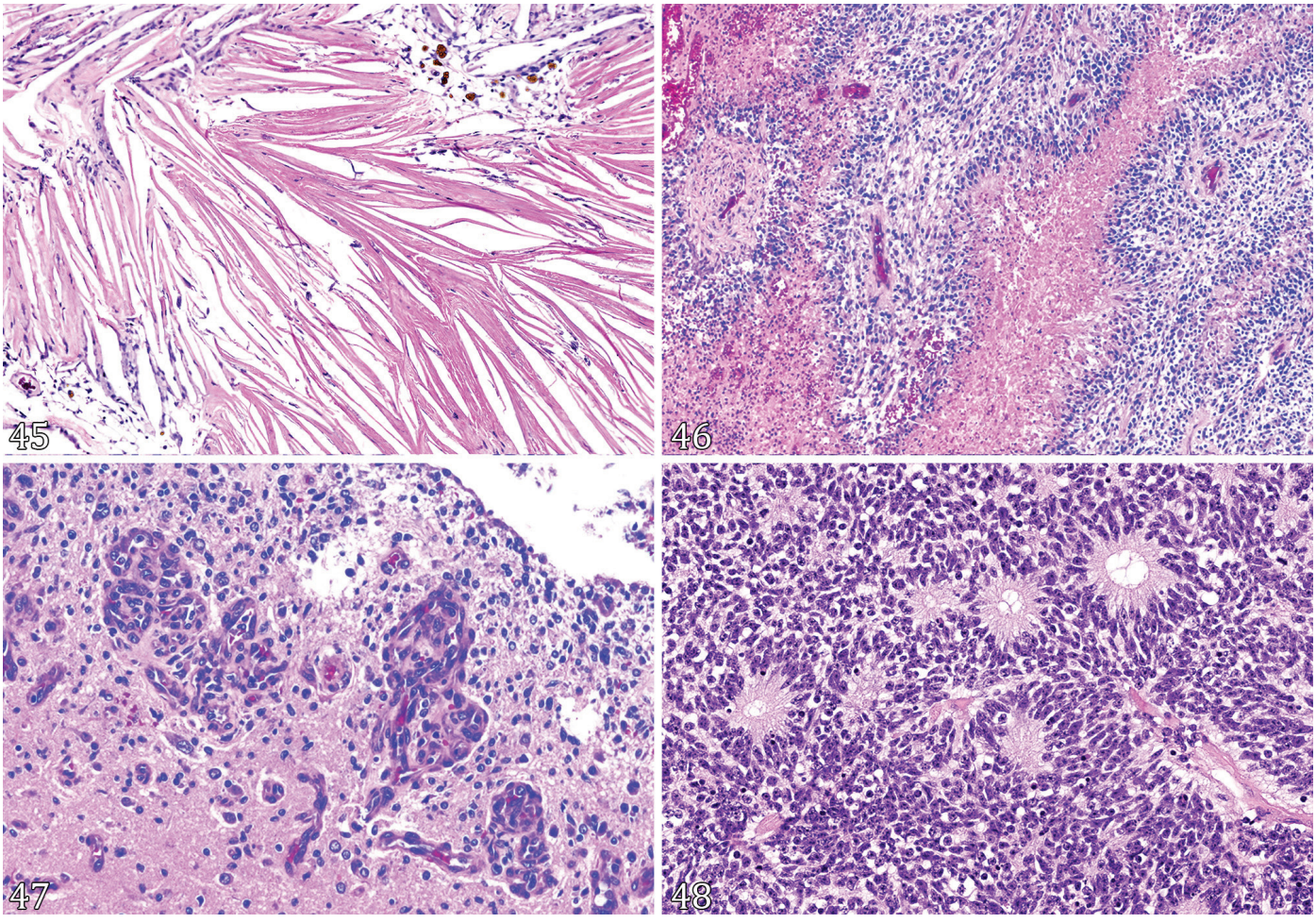

Fig.45-48. (**45**) Cholesterol granuloma; choroid plexus of the lateral ventricle; brain; equine. Shape analogy: Acicular clefts. The parallel needle-shaped clefts are characteristic of cholesterol clefts. HE, obj.20x. (**46**) Astrocytoma, high grade; brain; canine. Shape analogy: serpiginous tracks. Area of necrosis in a serpiginous pattern with pseudo-palisading neoplastic cells are characteristic of high-grade gliomas. HE, obj.10x. (**47**) Astrocytoma, high grade; brain; canine. Shape analogy: Glomeruloid vessels. These are microvascular proliferations along the periphery of the tumor that resemble renal glomeruli. HE, obj.20x. (**48**) Medulloepithelioma; eye; equine. Shape analogy: Rosettes. Neoplastic cells are arranged in a halo of neuroblastic cells around a nearly empty central lumen containing fine cytoplasmic extensions (Flexner-Wintersteiner rosettes). HE, obj.20x.

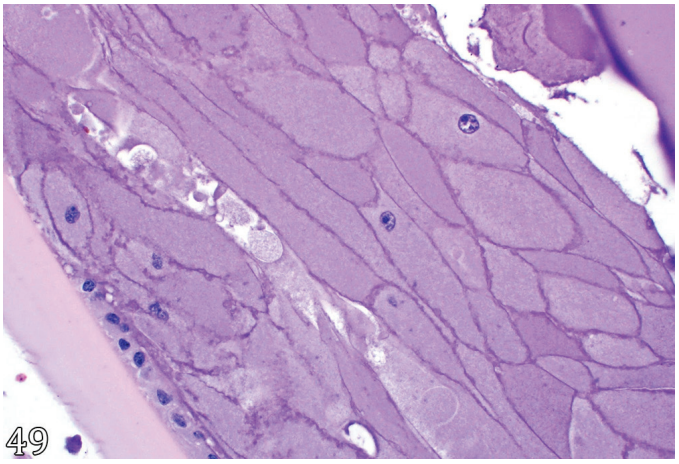

Fig.49. Cataract; eye; canine. Shape analogy: Bladder cells. Lens fibers are swollen with abundant eosinophilic cytoplasm and retained nuclei. HE, obj.40x. Photo courtesy: Dr. Laura Bryan, Texas A&M University.

Flexner-Wintersteiner rosettes are characterized by a halo of neuroblastic cells around a nearly empty central lumen containing fine cytoplasmic extensions (Wippold & Perry 2006). Retinoblastomas, pinealomas, and medulloepitheliomas (Fig.48) are examples of tumors that may contain Flexner-Wintersteiner rosettes (Wippold & Perry 2006). Different from the previously cited examples, an ependymal rosette contains an empty lumen that resembles a tubular lumen (Wippold & Perry 2006). Ependymal rosettes provide strong evidence of ependymal differentiation, although they occur only in well-differentiated ependymomas (Higgins et al. 2017). Lastly, perivascular rosettes, also known as pseudorosettes, comprise a halo of cells surrounding a blood vessel core (Wippold & Perry 2006). In cases of ependymoma, perivascular rosettes are more common than ependymal rosettes (Higgins et al. 2017) although they are not specific and can be observed in various neural tumors.

Special senses

Bladder cells. Bladder cells (in Portuguese: *células-bolha*) are a commonly described histologic feature of cataracts (Grahn et al. 2019). These cells are also called Wedl cells, named after Austrian pathologist Carl Wedl who first described them (Wedl 1861). The German word for bladder is "blase" which can also be translated to mean bubble or blister. Bladder cells are easily likened to bubbles. Histologically, they have abundant pale, granular to foamy cytoplasm (Fig.49). Bladder cells are hyperplastic nucleated lens epithelial cells that undergo hydropic degeneration and are thought to form as an attempt to regenerate lens fibers (Wilcock & Njaa 2016).

Conflict of interest statement.- The authors declare no conflicts of interest.

REFERENCES

Abdul-Aziz T. & Barnes H.J. 2018a. Avian keratoacanthoma in broiler chickens, p.275. In: Ibid. (Eds), Gross Pathology of Avian Diseases. AAAP, Florida.

Abdul-Aziz T. & Barnes H.J. 2018b. Histomoniasis, p.160-164. In: Ibid. (Eds), Gross Pathology of Avian Diseases. AAAP, Florida.

Ahmed A., Wojcik E.M., Ananthanarayanan V., Mulder L. & Mirza K.M. 2019. Learning styles in pathology: a comparative analysis and implications for learner-centered education. Acad. Pathol. 6:1-7. <https://dx.doi.org/10.1177/2374289519852315>

Anthony J.A., Waldner C., Grier C. & Laycock A. 2010. A survey of equine oral pathology. J. Vet. Dentistry 27(1):12-15. <https://dx.doi.org/10.1177/089875641002700102> <PMid:20469790>

Araújo V.O., Oliveira Neto T.S., Simões S.V., Silva T.K.F., Riet-Correa F. & Lucena R. 2017. Primary photosensitization and contact dermatitis caused by *Malachra fasciata* Jacq. N.V. (Malvaceae) in sheep. Toxicon 138:184-187. <https://dx.doi.org/10.1016/j.toxicon.2017.09.009> <PMid:28918228>

Atkinson V.T., Dickson W., Harbaugh W.H., Hickman R.W., Law J., Lowe W.H., Mohler J.R., Murray A.J., Pearson L., Ransom B.H., Salmon D.E., Smith T. & Trumbower M.R. 1909. Special Report on Disease of Cattle. Government Printing Office, Department of Agriculture, USA, p.414-418.

Bardagí M., Fondati A., Fondevila D. & Ferrer L. 2003. Ultrastructural study of cutaneous lesions in feline eosinophilic granuloma complex. Vet. Dermatol. 14(6):297-303. <https://dx.doi.org/10.1111/j.1365-3164.2003.00357.x> <PMid:14678441>

Barros R.R., Irigoyen L.F., Kommers G.D., Rech R.R., Fighera R.A. & Barros C.S.L. 2006. Poisoning by *Ramaria flavo-brunnescens* (*Clavariaceae*) in cattle. Pesq. Vet. Bras. 26(7):87-96. <https://dx.doi.org/10.1590/S0100-736X2006000200005>

Barthold S.W., Griffey S.M. & Percy D.H. 2016. Mouse, p.1-118. In Ibid. (Eds), Pathology of Laboratory Rodents and Rabbits. 4th ed., Wiley Blackwell, Ames.

Baverud V., Franklin A., Gunnarsson A., Gustafsson A. & Hellander-Edman A. 1998. *Clostridium difficile* associated with acute colitis in mares when their foals are treated with erythromycin and rifampicin for *Rhodococcus equi* pneumonia. Equine Vet. J. 30(6):482-488. <https://dx.doi.org/10.1111/j.2042-3306.1998.tb04523.x> <PMid:9844966>

Beasley V.R., Dahlem A.M., Cook W.O., Valentine W.M., Lovell R.A., Hooser S.B., Harada K., Suzuki M. & Carmichael W.W. 1989. Diagnostic and clinically important aspects of cyanobacterial (blue-green algae) toxicoses. J. Vet. Diagn. Invest. 1(4):359-365. <https://dx.doi.org/10.1177/104063878900100417> <PMid:2518710>

Blome S., Staubach C., Henke J., Carlson J. & Beer M. 2017. Classical swine fever - an updated review. Viruses 9(4):86. <https://dx.doi.org/10.3390/v9040086> <PMid:28430168>

Bowman D.B. 2014. Helminths, p.122-240. In: Bowman D.B. (Ed.), Georgis' Parasitology for Veterinarians. 10th ed. Elsevier, Saint Louis.

Breshears M.A & Confer A.W. 2017. The urinary system, p.621-637. In: Zachary J.F. (Ed.), Pathologic Basis of Veterinary Disease. 6th ed. Elsevier, Saint Louis.

Bridges C.H. & Emmons C.W. 1961. A phycomycosis of horsed caused by *Hyphomyces destruens*. J. Am. Vet. Med. Assoc. 138:579-589.

Brookins M., Rajeev S., Thornhill T., Kreinheder K. & Miller D. 2008. Mandibular and maxillary osteomyelitis and myositis in a captive herd of red kangaroos (*Macropus rufus*). J. Vet. Diag. Invest. 20(6):846-849. <https://dx.doi.org/10.1177/104063870802000627> <PMid:18987245>

Brown C.A., Jeong K.S., Poppenga R.H., Puschner B., Miller D.M., Ellis A.E., Kang K.I., Sum S., Cistola A.M. & Brown S.A. 2007. Outbreaks of renal failure associated with melamine and cyanuric acid in dogs and cats in 2004 and 2007. J. Vet. Diagn Invest. 19(5):525-531. <https://dx.doi.org/10.1177%2F104063870701900510> <PMid:17823396>

Campo M., Moar H., Sartirana M., Kennedy I. & Jarrett W. 1985. The presence of bovine papillomavirus type 4 DNA is not required for the progression to, or the maintenance of the malignant state in cancers of the alimentary canal in cattle. EMBO J. 4(7):1819-1825. <PMid:2992946>

Campo M., Moar M.H., Jarrett W.F. & Laird H.M. 1980. A new papillomavirus associated with alimentary cancer in cattle. Nature 286(5769):180-182. <https://dx.doi.org/10.1038/286180a0> <PMid:6250043>

Campo M.1997. Bovine papillomavirus and cancer. Vet. J.154(3):175-188. <https://dx.doi.org/10.1016/s1090-0233(97)80019-6> <PMid:9414951>

Caserto B.G. 2013. A comparative review of canine and human rhabdomyosarcoma with emphasis on classification and pathogenesis. Vet. Pathol. 50(5):806-826. <https://dx.doi.org/10.1177/0300985813476069> <PMid:23439712>

Chen Y., Quinn J.C., Weston L.A. & Loukopoulos P. 2019. The aetiology, prevalence and morbidity of outbreaks of photosensitisation in livestock: a review. PLoS One 14(2):e0211625. <https://dx.doi.org/10.1371/journal.pone.0211625> <PMid:30811417>

Cianciolo R.E. & Mohr F.C. 2016. Urinary system, p.376-464. In: Maxie M.G. (Ed.), Jubb, Kennedy, and Palmer's Pathology of Domestic Animals. Vol.2. 6th ed. Elsevier, St. Louis.

Cooper B.J. & Valentine B.A. 2017. Tumors of muscle, p.425-466. In: Meuten D.J. (Ed.), Tumors in Domestic Animals. 5th ed. Wiley Blackwell, Ames.

Corda A., Dessì G., Varcasia A., Carta S., Tamponi C., Sedda G., Scala M., Marchi B., Salis F., Scala A. & Parpaglia M.L.P. 2020. Acute visceral cysticercosis caused by *Taenia hydatigena* in lambs: ultrasonographic findings. *Parasit. Vectors* 13:568. <https://dx.doi.org/10.1186/s13071-020-04439-x>

Craig L.E., Dittmer K.E. & Thompson K.G. 2016. Mandibular ostomyelitis, p.102-103. In: Maxie M.G. (Ed.), Jubb, Kennedy, and Palmer's Pathology of Domestic Animals. Vol.1. 6th ed. Elsevier, St. Louis.

Craig L.E., Kinsella J.M., Lodwick L.J., Cranfield M.R. & Strandberg J.D. 1998. *Gongylonema macrogubernaculum* in captive African squirrels (*Funisciurus substriatus* and *Xerus erythropus*) and lion-tailed macaques (*Macaca Silenus*). J. Zoo Wildl. Med. 29(3):331-337. <PMid:9809609>

Cullen J.M. & Stalker M.J. 2016. Liver and biliary system, p.258-352. In: Maxie M.G. (Ed.), Jubb, Kennedy, and Palmer's Pathology of Domestic Animals. Vol.2. 6th ed. Elsevier, St. Louis.

D'Angelo A., Bellino C., Alborali G.L., Borrelli A., Capucchio M.T., Casalone C., Crescio M.I., Mattalia G.L. & Jaggy A. 2006. Aortic thrombosis in three calves with *Escherichia coli sepsis*. J. Vet. Intern. Med. 20(5):1261-1263. <https://dx.doi.org/10.1111/j.1939-1676.2006.tb00736.x> <PMid:17063730>

Datta S.C.A. 1933. The etiology of bursati. Indian J. Vet. Sci. 3:217-236.

Diab S.S., Rodriguez-Bertos A. & Uzal F.A. 2013. Pathology and diagnostic criteria of *Clostridium difficile* enteric infection in horses. Vet. Pathol. 50(6):1028-1036. <https://dx.doi.org/10.1177/0300985813489039> <PMid:23686768>

Döbereiner J., Tokarnia C.H., Canella C.F.C. 1967. Ocorrência de hematúria enzoótica e de carcinomas epidermóides no trato digestivo superior em bovinos no Brasil. Pesq. Agropec. Bras. 2(1):489-504.

Domingo M., Vidal E. & Marco A. 2014. Pathology of bovine tuberculosis. Res. Vet. Sci. 97(Supl.):S20-S29. <https://dx.doi.org/10.1016/j.rvsc.2014.03.017> <PMid:24731532>

Eberhard M.K. 2014. Histopathologic diagnosis, p.426. In: Bowman D.D. (Ed.), Georgis' Parasitology for Veterinarians. 10th ed. Elsevier, St. Louis.

Edwards E.E., Garner B.C., Williamson L.H., Storey B.E. & Sakamoto K. 2016. Pathology of *Haemonchus contortus* in New World camelids in the southeastern United States: a retrospective review. J. Vet. Diagn. Invest. 28(2):105-109. <https://dx.doi.org/10.1177/1040638716628587> <PMid:26965230>

Faccin T.C., Masuda E.K., Piazer J.V.M., Melo S.M.P. & Kommers G.D. 2017. Annular stenotic oesophageal squamous cell carcinoma in cattle exposed naturally to bracken fern (*Pteridium arachnoideum*). J. Comp. Pathol. 157(2/3):174-180. <https://dx.doi.org/10.1016/j.jcpa.2017.07.008> <PMid:28942300>

Fairley R.A. 1991. Collagenolysis: 'It ain't easy being pink'. Vet. Pathol. 28:96-97. <https://dx.doi.org/10.1177/030098589102800118> <PMid:2017836>

Fernandez C.J., Scott D.W. & Erb H.N. 2000. Staining abnormalities of dermal collagen in eosinophil or neutrophil-rich inflammatory dermatoses of horses and cats demonstrated with Masson's trichrome stain. Vet. Dermatol. 11(1):43-48. <https://dx.doi.org/10.1046/j.1365-3164.2000.00172.x>

Gelberg H.B. 2017. Alimentary system and the peritoneum, omentum, mesentery, and peritoneal cavity, p.374-380. In: Zachary J.F. (Ed.), Pathologic Basis of Veterinary Disease. 6th ed. Elsevier, St. Louis.

Giaretta P.R., Panziera W., Galiza G.J.N., Brum J.S., Bianchi R.M., Hammerschmitt M.E., Bazzi T. & Barros C.S.L. 2014. Seneciosis in cattle associated with photosensitization. Pesq. Vet. Bras. 34(5):427-432. <https://dx.doi.org/10.1590/S0100-736X2014000500007>

Goldschmidt M.H. & Golschmidt K.H. 2017. Epithelial and melanocytic tumors of the skin, p.88-141. In: Meuten D.J. (Ed.), Tumors in Domestic Animals. 5th ed. Wiley Blackwell, Ames.

Gopinath D. 2018. Splendore-Hoeppli phenomenon. J. Oral Maxillfac. Pathol. 22(2):161-162. <https://dx.doi.org/10.4103/jomfp.JOMFP_79_18> <PMid:30158765>

Grahn B.G., Peiffer R. & Wilcock B. 2019. Histologic manifestations of acquired and inherited diseases of the lens, p.296. In: Ibid. (Eds), Histologic Basis of Ocular Disease in Animals. John Wiley and Sons, Hoboken, NJ.

Grist A. 2008. Conditions encountered at bovine *post mortem* inspection (non parasitic), p.160-239. In: Ibid. (Ed.), Bovine Meat Inspection. 2nd ed. Nottingham University Press, Nottingham.

Gross T.L., Ihrke P.J., Walder E.J. & Affolter V.K. 2005a. Diseases of the adnexa, p.518-536. In: Ibid. (Eds), Skin Diseases of the Dog and Cat: clinical and histopathological diagnosis. 2nd ed. Blackwell Publishing, Oxford.

Gross T.L., Ihrke P.J., Walder E.J. & Affolter V.K. 2005b. Infectious nodular and diffuse granulomatous and pyogranulomatous diseases of the dermis, p.272-319. In: Ibid. (Eds), Skin Diseases of the Dog and Cat: clinical and histopathological diagnosis.2nd ed. Blackwell Publishing, Oxford.

Gross T.L., Ihrke P.J., Walder E.J. & Affolter V.K. 2005c. Nodular and diffuse diseases of the dermis with prominent eosinophils, neutrophils, or plasma cells, p.356-357. In: Ibid. (Eds), Skin Diseases of the Dog and Cat: clinical and histopathological diagnosis.2nd ed. Blackwell Publishing, Oxford.

Higgins R.J., Bollen A.W., Dickinson P.J. & Llonch S.S. 2017. Tumors of the nervous system, p.834-891. In: Meuten D.J. (Ed.), Tumors in Domestic Animals. 5th ed. Wiley Blackwell, Ames.

Hilton H., Aleman M., Textor J., Nieto J. & Pevec W. 2008. Ultrasound-guided balloon thrombectomy for treatment of aorto-iliac-femoral thrombosis in a horse. J. Vet. Intern. Med. 22(3):679-683. <https://dx.doi.org/10.1111/j.1939-1676.2008.0095.x> <PMid:18466242>

Hobday M.M., Pachtinger G.E., Drobatz K.J. & Syring R.S. 2014. Linear versus non-linear gastrointestinal foreign bodies in 499 dogs: clinical presentation, management and short-term outcome. J. Small Anim. Pract. 55(11):560-565. <https://dx.doi.org/10.1111/jsap.12271> <PMid:25352109>

Hoeppli R. 1932. Histological observations in experimental schistosomiasis Japónica. Chin. Med. J. 46(12):1179-1186.

Hussein M.R. 2008. Mucocutaneous Splendore-Hoeppli phenomenon. J. Cutan. Pathol. 35(11):979-988. <https://dx.doi.org/10.1111/j.1600-0560.2008.01045.x> <PMid:18976399>

Jarrett W., McNeil P., Grimshaw W., Selman I. & McIntyre W. 1978. High incidence area of cattle cancer with a possible interaction between an environmental carcinogen and a papilloma virus. Nature 274(5668):215-217. <https://dx.doi.org/10.1038/274215a0> <PMid:210386>

Jiang H., Wang D., Wang D., Wang J., Zhu S., She R., Ren X., Tian J., Quan R., Hou L., Li Z., Chu J., Guo Y., Xi Y., Song H., Yuan F., Wei L. & Liu J. 2019. Induction of porcine dermatitis and nephropathy syndrome in piglets by infection with porcine circovirus type 3. J. Virol. 93(4):e02045-18. <https://dx.doi.org/10.1128/JVI.02045-18>

Jones T.C., Hunt R.D. & King N.W. 1997. Actinomycosis, p.482-484. In: Ibid. (Eds), Veterinary Pathology. 6th ed. Williams and Wilkins, Baltimore.

Keel M.K. & Songer J.G. 2006. The comparative pathology of *Clostridium difficile*-associated disease. Vet. Pathol. 43(3):225-240. <https://dx.doi.org/10.1354%2Fvp.43-3-225> <PMid:16672570>

Knaust J., Hadlich F., Weikard R. & Kuehn C. 2016. Epistatic interactions between at least three loci determine the "rat-tail" phenotype in cattle. Genet. Sel. Evol. 48:26. <https://dx.doi.org/10.1186/s12711-016-0199-8> <PMid:27037038>

Koehler J.W., Miller A.D., Miller R., Porter B., Aldape K., Beck J., Brat D., Cornax I., Corps K., Frank C., Giannini C., Horbinski C., Huse J.T., O'Sullivan G., Rissi D.R., Simpson M., Woodlard K., Shih J.H., Mazcho C., Gilbert M.R. & LeBlanc A.K. 2018. A revised diagnostic classification of canine glioma: towards validation of the canine glioma patient as a naturally occurring preclinical model for human glioma. Neuropathol. Exp. Neurol. 77(11):1039-1054. <https://dx.doi.org/10.1093/jnen/nly085> <PMid:30239918>

Ladeira S.L.R. 2007. Lechiguana, p.325-330. In: Riet-Correa F., Schild A.L., Lemos R.A.A. & Borges J.R.J. (Eds), Doenças de Ruminantes e Eqüídeos. Vol.1. 3rd ed. Pallotti, Santa Maria.

Laffort-Dassot C., Beco L. & Carlott N.D. 2002. Case report: follicular dysplasia in five Weimaraners. Vet. Dermatol. 13(5):253-260. <https://dx.doi.org/10.1046/j.1365-3164.2002.00302.x> <PMid:12358609>

Lake-Bakaar G.A., Johnson E.G. & Griffiths L.G. 2012. Aortic thrombosis in dogs: 31 cases (2000-2010). J. Am. Vet. Med. Assoc. 241(7):910-915. <https://dx.doi.org/10.2460/javma.241.7.910> <PMid:23013504>

Lange C.E., Tobler K., Lehner A., Grest P., Welle M.M., Schwarzwald C.C. & C. Favrot C. 2012. EcPV2 DNA in equine papillomas and in situ and invasive squamous cell carcinomas supports papillomavirus etiology. Vet. Pathol. 50(4):686-692. <https://dx.doi.org/10.1177/0300985812463403> <PMid:23064881>

Leal P.V., Pupin R.C., Lima S.C., Melo G.K., Araújo M.A., Gomes D.C., Barros C.S. & Lemos R.A. 2017. Ingestion of the pods of *Enterolobium contortisiliquum* causes hepatogenous photosensitization in cattle. Toxicon 131:6-10. <https://dx.doi.org/10.1016/j.toxicon.2017.03.009> <PMid:28300579>

Lecha M., Puy H. & Deybach J. C. 2009. Erythropoietic protoporphyria. Orphanet J. Rare Dis. 4:19. <https://dx.doi.org/10.1186/1750-1172-4-19> <PMid:19744342>

Libertin C.R., Reza M., Peterson J.H., Lewis J. & Hata J.D. 2017. Human *Gongylonema pulchrum* infection: esophageal symptoms and need for prolonged albendazole therapy. Am. J. Trop. Med. Hyg. 96(4):873-875. <https://dx.doi.org/10.4269/ajtmh.16-0852> <PMid:28138043>

Lucena R., Rissi D., Kommers G., Pierezan F., Oliveira-Filho J., Macedo J., Flores M. & Barros C.S.L. 2011. A retrospective study of 586 tumours in Brazilian cattle. J. Comp. Pathol. 145(1):20-24. <https://dx.doi.org/10.1016/j.jcpa.2010.11.002> <PMid:21247583>

Lurie H. 1971. Sporotrichosis: morphology of asterois bodies, p.647-654. In: Baker R.D. (Ed.), Human Infection with Fungi, Actinomyces, and Algae. Springer-Verlag. Heidelberg-Berlin.

Madewell B.R., Tang Y.J., Jang S., Madigan J.E., Hirsh D.C., Gumerlock P.H. & Silva Jr J. 1995. Apparent outbreaks of *Clostridium difficile*-associated diarrhea in horses in a veterinary medical teaching hospital. J. Vet. Diagn. Invest. 7(3):343-346. <https://dx.doi.org/10.1177/104063879500700308> <PMid:7578449>

Martins T.B., Kommers G.D., Trost M.E., Inkelmann M.A., Fighera R.A. & Schild A.L. 2012. A comparative study of the histopathology and immunohistochemistry of pythiosis in horses, dogs and cattle. J. Comp. Pathol. 146(2/3):122-131. <https://dx.doi.org/10.1016/j.jcpa.2011.06.006> <PMid:21824626>

Masuda E., Kommers G., Martins T., Barros C. & Piazer J. 2011. Morphological factors as indicators of malignancy of squamous cell carcinomas in cattle exposed naturally to bracken fern (*Pteridium aquilinum*). J. Comp. Pathol. 144(1):48-54. <https://dx.doi.org/10.1016/j.jcpa.2010.04.009> <PMid:20542519>

Mattes F.M., McLaughlin J.E., Emery V.C., Clark D.A. & Griffiths P.D. 2000. Histopathological detection of owl's eye inclusions is still specific for cytomegalovirus in the era of human herpesviruses 6 and 7. J. Clin. Pathol. 53(8):612-614. <https://dx.doi.org/10.1136/jcp.53.8.612> <PMid:11002765>

Mauldin E.A. & Peters-Kennedy J. 2016. Integumentary system, p.509-736. In: Maxie M.G. (Ed.), Jubb, Kennedy, and Palmer's Pathology of Domestic Animals. Vol.1. 6th ed. Elsevier, St. Louis.

Meuten D.J. & Meuten T.L.K. 2017. Tumors of the urinary system, p.681. In: Meuten D.J. (Ed.), Tumors in Domestic Animals. 5th ed. Wiley Blackwell, Ames.

Miller M.A. & Dunstan R.W. 1993. Seasonal flank alopecia in Boxers and Airedale Terriers: 24 cases (1985-1992). J. Am. Vet. Med. Assoc. 203(11):1567-1572. <PMid:8288480>

Miller R.I. & Campbell R.S.F. 1984 The Comparative pathology of equine cutaneous phycomycosis. Vet. Pathol. 21(3):25-332. <https://dx.doi.org/10.1177/030098588402100310> <PMid:6730223>

Misago N., Inoue T., Koba S., & Narisawa Y. 2013. Keratoacanthoma and other types of squamous cell carcinoma with crateriform architecture: classification and identification. J. Dermatol. 40(6):443-452. <https://dx.doi.org/10.1111/1346-8138.12104> <PMid:23414327>

Morton J.F. 1994. Lantana, or red sage (*Lantana camara* L., [Verbenaceae]), notorious weed and popular garden flower; some cases of poisoning in Florida. Econ. Bot. 48(3):259-270. <https://dx.doi.org/10.1007/BF02862327>

Munday J.S., Brennan M.M., Jaber A.M. & Kiupel M. 2006. Ovine intestinal adenocarcinomas: histologic and phenotypic comparison with human colon cancer. Comp. Med. 56(2):136-141. <PMid:16639981>

Munday J.S., Lohr C.V. & Kiupel M. 2017.Tumors of the alimentary tract, p.499-601. In: Meuten D.J. (Ed.), Tumors in Domestic Animals. 5th ed. Wiley Blackwell, Ames.

Murphy B.G., Bell C.M. & Soukup J.W. 2020. Odontogenic tumors, p.91-104. In: Ibid. (Eds), Veterinary Oral and Maxillofacial Pathology. Wiley Blackwell, Hoboken.

Myers G.H. & Taylor R.F. 1989. Ostertagiasis in cattle. J. Vet. Diagn. Invest. 1(2):195-200. <https://dx.doi.org/10.1177%2F104063878900100225>

Newbold F. 1846. Summary of the geology of Southern India. J. R. Asiat. Soc. Great Britain and Ireland. 8(1846):138-271.

Nilubol D., Pattanaseth T. & Boonsri K. 2009. Melamine- and cyanuric acid-associated renal failure in pigs in Thailand. Vet. Pathol. 46(6):1156-1159. <https://dx.doi.org/10.1354%2Fvp.08-VP-0233-N-FL> <PMid:19605898>

Njaa B.L., Panciera R.J., Clark E.G. & Lamm C.G. 2012. Gross lesions of alimentary disease in adult cattle. Vet. Clin. N. Am., Food. Anim. Pract. 28(3):483-513. <https://dx.doi.org/10.1016/j.cvfa.2012.07.009> <PMid:23101672>

Omobowale T.O., Otuh P. I., Ogunro B.N., Adejumobi O.A., & Ogunleye A.O. 2017. Infective endocarditis in dogs: a review. Eur. J. Pharm. Med. Res. 4(8):103-109.

Opriessnig T. & Coutinho T.A. 2019. Erysipelas, p.835-843. In: Zimmerman J.J., Karrier L.A., Ramirez A., Schwartz K.J., Stevenson G.W. & Zhang J. (Eds), Diseases of Swine. 11th ed. Wiley-Blackwell, St. Louis.

O'Toole D. & Raisbeck M.F. 1995. Pathology of experimentally induced chronic selenosis (alkali disease) in yearling cattle. J. Vet. Diagn. Invest. 7(3):364-373. <https://dx.doi.org/10.1177/104063879500700312> <PMid:7578453>

Panziera W., Gonçalves M.A., Oliveira L.G.S., Lorenzett M.P., Reis M., Hammerschmitt M.E., Pavarini S.P. & Driemeier D. 2017. Intoxicação por *Senecio brasiliensis* em bezerros: padrão e evolução de lesões hepáticas. Pesq. Vet. Brasil. 37(1):8-16. <https://dx.doi.org/10.1590/s0100-736x2017000100002>

Payne C.L., Dark M.J., Conway J.A. & Farina L.L. 2017. A retrospective study of the prevalence of calcium oxalate crystals in veterinary *Aspergillus* cases. J. Vet. Diagn. Invest. 29(1):51-58. <https://dx.doi.org/10.1177/1040638716672254> <PMid:27852812>

Peters M.S., Schroeter A.L. & Gleich G.L. 1983. Immunofluorescence identification of eosinophil granule major basic protein in the flame figures of Wells' syndrome. Brit. J. Dermatol. 109(2):141-148. <https://dx.doi.org/10.1111/j.1365-2133.1983.tb07074.x> <PMid:6347236>

Puschner B., Poppenga R.H., Lowenstine L.J., Filigenzi M.S. & Pesavento P.A. 2007. Assessment of melamine and cyanuric acid toxicity in cats. J. Vet. Diagn. Invest. 19(6):616-624. <https://dx.doi.org/10.1177%2F104063870701900602> <PMid:17998549>

Riet-Correa F., Méndez M.C., Schild A.L., Ribeiro G.A. & Almeida S.M. 1992. Bovine focal proliferative fibrogranulomatous panniculitis (lechiguana) associated with *Pasteurella granulomatis*. Vet. Pathol. 29(2):93-103. <https://dx.doi.org/10.1177/030098589202900201> <PMid:1632062>

Robinson W.F. & Robinson N.A. 2016. Cardiovascular system, p.1-101. In: Maxie M.G. (Ed.), Jubb, Kennedy, and Palmer's Pathology of Domestic Animals. Vol.3. 6th ed Elsevier, St. Louis.

Sato Y., Inoue N., Ishikawa T., Ishibashi R., Obata M., Aoki H., Atsumi T. & Komaru A. 2013. Pearl microstructure and expression of shell matrix protein genes MSI31 and MSI60 in the pearl sac epithelium of *Pinctada fucata* by *in situ* hybridization. PLoS One 8. <https://dx.doi.org/10.1371/journal.pone.0052372> <PMid:23341897>

Schlafer D.H. & Foster R.A. 2015. Female genital system, p.358-464. In: Maxie M.G. (Ed.), Jubb, Kennedy, and Palmer's Pathology of Domestic Animals. Vol.3. 6th ed. Elsevier, St. Louis.

Scott D. & Miller W. 2010. Diagnostic methods, p.124. In: Ibid. (Eds), Equine Dermatology. 2nd ed. W.B. Saunders, Missouri.

Scott D.W. 2018. Color Atlas of Farm Animal Dermatology. 2nd. Wiley Blackwell, Hoboken, p.185.

Seawright A.A. 1982. Photosensitisation, p.6. In: Ibid. (Ed.), Animal Health in Australia. Volume 2: Chemical and Plant Poisons. Australian Government Publishing Service, Canberra.

Segales J. 2012. Porcine circovirus type 2 (PCV2) infections: clinical signs, pathology and laboratory diagnosis. Virus Res. 164(1/2):10-19. <https://dx.doi.org/10.1016/j.virusres.2011.10.007> <PMid:22056845>

Smith B.J., Anderson B.G., Smith S.A. & Chew D.J. 1990. Early effects of ethylene glycol on the ultrastructure of the renal cortex in dogs. Am. J. Vet. Res. 51(1):89-96. <PMid:2301826>

Smith F. 1879. Bursattee. Vet. J. Ann. Comp. Pathol. 9:295-374.

Souto M., Kommers G., Barros C.S.L., Piazer J. & Rech R. 2006. Neoplasias do trato alimentar superior de bovinos associadas ao consumo espontâneo de samambaia (*Pteridium aquilinum*). Pesq. Vet. Bras. 26(2):112-122. <https://dx.doi.org/10.1590/S0100-736X2006000200009>

Splendore A. 1908. Sobre a cultura d'uma nova especie de cogumello pathogenico (Sporotrichose de Splendore). Revta Soc. Sci. São Paulo 3:62.

Taghavi K., Kirkpatrick J. & Mirjalili SA. 2016. The horseshoe kidney: surgical anatomy and embryology. Rev. J. Pediatr. Urol. 12(5):275-280. <https://dx.doi.org/10.1016/j.jpurol.2016.04.033> <PMid:27324557>

Tessele B., Vielmo A., Hammerschmitt M. & Barros C.S.L. 2014. Actinomicose atípica em bovinos. Pesq. Vet. Bras. 34(7):663-666. <https://dx.doi.org/10.1590/S0100-736X2014000700010>

Thompson J. & Young J. 1986. The Florida ''horse-leech'' 1893/1894. 10th and 11th Annual Report of the Bureau of Animal Industry, USA, p.97-98.

Tokarnia C.H., Brito M.F., Barbosa J.D., Peixoto P.V. & Döbereiner J. 2012a. *Senecio* spp., p.177-191. In: Ibid. (Eds), Plantas Tóxicas do Brasil para Animais de Produção. 2ª ed. Editora Helianthus, Rio de Janeiro.

Tokarnia C.H., Brito M.F., Barbosa J.D., Peixoto P.V. & Döbereiner J. 2012b. Plantas/micotoxinas fotossensibilizantes, p.305-348. In: Ibid. (Eds), Plantas Tóxicas do Brasil para Animais de Produção. 2nd ed. Helianthus, Rio de Janeiro.

Towersey L., Martins-Ede C., Londero A.T., Hay R.J., Soares-Filho P.J., Takiya C.M., Martins C.C. & Gompertz O.F. 1993. *Dermatophilus congolensis* human infection. J. Am. Acad. Dermatol. 29(2):351-354. <https://dx.doi.org/10.1016/0190-9622(93)70194-X>

Trost M.E., Kommers G.D., Barros C.S.L & Schild A.L. 2009. Patogênese das lesões associadas à intoxicação por *Ramaria flavo-brunnescens* em bovinos. Pesq. Vet. Bras. 29(7):533-544. . <https://dx.doi.org/10.1590/S0100-736X2009000700007>

Ueda Y., Aohagi Y. & Nakahara S. 2005. Distribution of protoporphyrin in female broiler chickens affected with protoporphyria. J. Vet. Med. Sci. 67(12):1289-1291. <https://dx.doi.org/10.1292/jvms.67.1289> <PMid:16397395>

Uzal F.A. & Diab S.S. 2015. Gastritis, enteritis, and colitis in horses. Vet. Clin. Equine 31(2):337-358. <https://dx.doi.org/10.1016/j.cveq.2015.04.006> <PMid:26048413>

Uzal F.A., Plattner B.L. & Hostetter J.N. 2016. Alimentary system, p.1-257. In: Maxie M.G. (Ed.), Jubb, Kennedy, and Palmer's Pathology of Domestic Animals. 6th ed. Vol.2. Elsevier, St. Louis.

Valli V.E., Jacobs R.M., Parodi A.L., Vernau W. & Moore P.F. 2002. Histological Classification of Hematopoietic Tumors of Domestic Animals. Armed Forces Institute of Pathology, Washington, DC. 190p.

Valli V.E.O., Kiupel M. & Bienzle D. 2016. Hematopoietic system, p.102-268. In: Maxie M.G. (Ed.), Jubb, Kennedy, and Palmer's Pathology of Domestic Animals. 6th ed. Vol 3. Elsevier, St. Louis.

Varaschin M.S., Wouters F. & Prado E.S. 1998. Porfiria eritropoética congênita em bovino no estado de Minas Gerais. Ciência Rural 28:695-698. <https://dx.doi.org/10.1590/S0103-84781998000400026>

Vitiello V., Burrai G.P., Agus M., Anfossi A.G., Alberti A., Antuofermo E., Rocca S., Tiziana Cubeddu T. & Pirino S. 2017. *Ovis aries* papillomavirus 3 in ovine cutaneous squamous cell carcinoma. Vet. Pathol. 54(5):775-782. <https://dx.doi.org/10.1177/0300985817705171> <PMid:28494708>

Wedl C. 1861. Lens - corp. vitr. III., p.65-67. In: Ibid. (Ed.), Atlas der pathologischen Histologie des Auges: Unter Mitwirkung des Herrn Prof. Dr. C. Stellwag von Carion herausgegeben von Prof. Dr. C. Wedl. Georg Wigland's Verlag, Leipzig.

Wells G. 1971. Recurrent granulomatous dermatitis with eosinophilia. Trans St. Johns Hosp. Dermatol. Soc. 57(1):46-56. <PMid:5570262>

Whitaker I.S., Rao J., Izadi D. & Butler P.E. 2004. Historical Article: *Hirudo medicinalis:* ancient origins of, and trends in the use of medicinal leeches throughout history. J. Oral Maxillofac. Surg. 42(2):133-137. <https://dx.doi.org/10.1016/S0266-4356(03)00242-0> <PMid:15013545>

Wiener D.J. 2021. Histologic features of hair follicle neoplasms and cysts in dogs and cats: a diagnostic guide. J. Vet. Diagn. Invest. 33(3):3. <https://dx.doi.org/10.1177/1040638721993565> <PMid:33666111>

Wilcock B.P. & Njaa B.L. 2016. Special senses, p.442. In: Maxie M.G. (Ed.), Jubb, Kennedy and, Palmer's Pathology of Domestic Animals. 6th. Vol.1. Elsevier, St. Louis.

Wilson W.G. 2005. Specific diseases, p.112-136. In: Ibid. (Ed.), Wilson's Practical Meat Inspection. 7th ed. Blackwell, Oxford.

Wippold F.J. & Perry A. 2006. Neuropathology for the neuroradiologist: rosettes and pseudorosettes. Am. J. Neuroradiol. 27(3):488-492. <PMid:16551982>

Wouters J., Waelkens E., Vandoninck S., Segaert S. & van den Oord J. 2015. Mass spectrometry of flame figures. Acta Derm. Venereol. 95(6):734-735. <https://dx.doi.org/10.2340/00015555-2050> <PMid:25613159>

Yhee J.Y., Brown C.A., Yu C.H., Kim J.H., Poppenga R. & Sur J.H. 2009. Retrospective study of melamine/cyanuric acid-induced renal failure in dogs in Korea between 2003 and 2004. Vet. Pathol. 46(2):348-354. <https://dx.doi.org/10.1354%2Fvp.46-2-348> <PMid:19261650>

Zaria L.T. & Amin J.D. 2004. Dermatophilosis, p.2026-2042. In: Coetzer J.A.W. & Tustin R.C. (Eds), Infectious Diseases of Livestock. Vol.3. Oxford University Press, New York.

Zhang H.M., Yan Y.P., Sun G.C., Hum H.X., Liu Z.F. & Feng Y.J. 2000. Cutaneous blood vessels in scent pigs. Plast. Reconstr. Surg. 106(7):1555-1565. <https://dx.doi.org/10.1097/00006534-200012000-00017> <PMid:11129185>